Published in "Angiogenesis 18(3): 327–345, 2015"
which should be cited to refer to this work.

An immature B cell population from peripheral blood serves as surrogate marker for monitoring tumor angiogenesis and anti-angiogenic therapy in mouse models

Ernesta Fagiani[1] · Ruben Bill[1] · Laura Pisarsky[1] · Robert Ivanek[1] · Curzio Rüegg[2] · Gerhard Christofori[1]

Abstract Tumor growth depends on the formation of new blood vessels (tumor angiogenesis) either from preexisting vessels or by the recruitment of bone marrow-derived cells. Despite encouraging results obtained with preclinical cancer models, the therapeutic targeting of tumor angiogenesis has thus far failed to deliver an enduring clinical response in cancer patients. One major obstacle for improving anti-angiogenic therapy is the lack of validated biomarkers, which allow patient stratification for suitable treatment and a rapid assessment of therapy response. Toward these goals, we have employed several mouse models of tumor angiogenesis to identify cell populations circulating in their blood that correlated with the extent of tumor angiogenesis and therapy response. Flow cytometry analyses of different combinations of cell surface markers that define subsets of bone marrow-derived cells were performed on peripheral blood mononuclear cells from tumor-bearing and healthy mice. We identified one cell population, $CD45^{dim}VEGFR1^{-}CD31^{low}$, that was increased in levels during active tumor angiogenesis in a variety of transgenic and syngeneic transplantation mouse models of cancer. Treatment with various anti-angiogenic drugs did not affect $CD45^{dim}VEGFR1^{-}CD31^{low}$ cells in healthy mice, whereas in tumor-bearing mice, a consistent reduction in their levels was observed. Gene expression profiling of $CD45^{dim}VEGFR1^{-}CD31^{low}$ cells characterized these cells as an immature B cell population. These immature B cells were then directly validated as surrogate marker for tumor angiogenesis and of pharmacologic responses to anti-angiogenic therapies in various mouse models of cancer.

Keywords Anti-angiogenic therapy · B cell · Biomarker · Cancer · Tumor angiogenesis

Abbreviations

PBMNC	Peripheral blood mononuclear cell
FGF	Fibroblast growth factor
PDGF	Platelet-derived growth factor
VEGF	Vascular endothelial growth factor
VEGFR	VEGF receptor
PlGF	Placental growth factor
HGF	Hepatocyte growth factor
TNFα	Tumor necrosis factor α
TGFβ	Transforming growth factor β
TAM	Tumor-associated macrophage
TEM	TIE2-expressing monocyte
CEC	Circulating endothelial cell
EPC	Endothelial progenitor cell
IL	Interleukin

Electronic supplementary material is available

✉ Gerhard Christofori
gerhard.christofori@unibas.ch

[1] Department of Biomedicine, University of Basel, Mattenstrasse 28, 4058 Basel, Switzerland

[2] Department of Medicine, Faculty of Science, University of Fribourg, Rue Albert Gockel 1, 1700 Fribourg, Switzerland

Introduction

The "angiogenic switch" is considered a hallmark of malignant tumor progression, mainly caused by a shift of the balance between positive and negative regulators of

angiogenesis to pro-angiogenic activities [1]. Specifically, neo-angiogenesis involves the sprouting, migration and proliferation of endothelial cells from preexisting blood vessels or the formation of capillary sprouts by intussusception [2, 3]. Angiogenesis is controlled by several soluble factors, such as placental growth factor (PlGF), fibroblast growth factors (FGFs), hepatocyte growth factor (HGF), angiopoietins, ephrins, semaphorins, interleukins and other chemokines [4] and, most importantly, vascular endothelial growth factor A (VEGF-A), the central player in both physiological and pathological angiogenesis [5–7]). Pro-angiogenic factors are produced by both neoplastic and stromal cells in the tumor microenvironment [8–11]. On the other hand, during the angiogenic switch, a number of endogenous angiogenesis inhibitors, such as thrombospondin, are reduced in their expression levels [12].

The search for valid biomarkers of the angiogenic switch and ongoing tumor angiogenesis has revealed that bone marrow-derived $CD45^{+}$ leukocytes infiltrating the tumor microenvironment can be used to assess patients' clinical outcome in melanoma and in colorectal, mammary, lung and ovarian carcinomas [13–17]. While several studies suggest an anti-tumorigenic role for leukocytes, a plethora of studies demonstrate a critical role for them in cancer initiation and progression [18, 19]. Notably, different leukocyte subsets have been shown to be involved in vascular remodeling and new blood vessel formation [20]. Importantly, innate immune cells have been clearly proved to be involved in the process of tumor angiogenesis mainly by their recruitment to the tumor site and the secretion of a cocktail of pro-angiogenic factors [21–27]. On the other hand, non-hematopoietic $CD45^{dim/negative}$ endothelial precursors cells (EPC) can be mobilized from the bone marrow and transported in the blood stream to the tumor site where they are incorporated into the wall of growing blood vessel, thus contributing to tumor angiogenesis [8]. However, due to the absence of highly specific cell surface markers used to identify EPCs, there are conflicting data whether and to what extent these cells are incorporated into the vessel wall and eventually contribute to tumor angiogenesis [8, 9, 28, 29].

Anti-angiogenic therapy mainly targets blood vessels in the tumor with the aim to impede tumor growth and metastasis formation. The critical role of the VEGF-A/VEGF receptor-2 (VEGFR-2) signaling axis in the onset of tumor angiogenesis has led to the development of several drugs targeting this pathway. An example is bevacizumab (Avastin®), a humanized antibody neutralizing VEGF-A with varying efficacy in different cancer types [30–32]. Apparently, in some cancer types, VEGF-A is not the only factor inducing tumor angiogenesis, such as in breast cancer. Moreover, interfering with VEGF-A signaling in most cases resulted in resistance development by the compensatory production of other angiogenic factors by tumor cells and/or stromal cells [33], for example, by tumor-infiltrating Th17 cells providing pro-angiogenic IL17 [34]. Thus, strategies to overcome resistance to single-targeted anti-angiogenic agents include the development of novel compounds that target tumor angiogenesis and thus tumor growth through multiple pathways [35].

Obviously, the possibility to monitor in a longitudinal and noninvasive manner ongoing tumor angiogenesis in patients and their responses to anti-angiogenic therapies would be beneficial for efficient anti-angiogenic cancer therapy. Hence, the discovery of reliable biomarkers seems essential to predict the response of anti-angiogenic therapy and the development of resistance to anti-angiogenic therapy in patients. An example is the measurement of circulating levels of VEGF-A, FGF-2, HGF and IL-8, which, however, reliably predicted survival only in some models [36]. Furthermore, levels of circulating endothelial cells (CECs) and EPCs increase in blood during tumor angiogenesis or other vascular diseases and, therefore, could also be employed as surrogate markers [8, 36–38]. In addition, as described above, bone marrow-derived cell populations also may have the potential to serve as surrogate markers for monitoring tumor angiogenesis and anti-angiogenic therapies.

Here, we report that the levels of a bone marrow-derived cell population, $CD45^{dim}VEGFR1^{-}CD31^{low}$, were increased in peripheral blood in a variety of mouse models of tumor angiogenesis in comparison with healthy mice. These high levels in tumor-bearing mice were reduced upon treatment with the anti-angiogenic compound PTK787/ZK222584 (PTK/ZK) that interfered with VEGF receptor signaling. Surprisingly, treatment for longer time periods re-established the levels of the cell population in the peripheral blood which correlated with therapy resistance and tumor regrowth. In contrast, long-term treatment using compounds that in addition to VEGF also inhibited FGF and PDGF (BIBF-1120, nintedanib) led to a significant decrease in the levels of $CD45^{dim}VEGFR1^{--}CD31^{low}$ cells in the blood of tumor mice as well as a reduction in tumor volume and microvessel densities. Gene expression profiling identified $CD45^{dim}VEGFR1^{-}CD31^{low}$ cells as an immature B cell population. Subsequent direct analysis validated the correlation between the levels of the immature B cell population in peripheral blood with ongoing tumor angiogenesis and with a response to anti-angiogenic therapies in different mouse models of cancer. This cell population thus may serve as surrogate marker for tumor angiogenesis and for the response to anti-angiogenic therapy.

Materials and methods

Mouse lines

All experimental procedures involving mice were approved by and conducted according to the guidelines and regulations of the local committees for animal care (The Swiss Federal Veterinary Office (SFVO) and the Cantonal Veterinary Office of Basel-Stadt, permit numbers 1878, 1907, 1908, 2137).

Generation and phenotypic characterization of Rip1-Tag2 (RT2) and MMTV-PyMT mice have been described previously [39–41]. In RT2 mice, tumor incidence was determined per mouse by counting of all macroscopically visible pancreatic tumors with a diameter above 1 mm and the tumor volume was calculated from the measured tumor diameter assuming a spherical tumor. In MMTV-PyMT mice, tumor volume per mouse was calculated as the total weight of all tumors dissected form each mouse. C57BL/6-Tg(ACTB-EGFP) mice [42] were provided by G. Holländer (University of Basel).

Tumor transplantation models

5×10^5 TRAMP-C1 cells [43] (provided by N. Greenberg, FHCRC, Seattle) were injected into the flank of 6-week-old C57BL/6 mice and grown for 3–4 weeks [29]. 5×10^5 Py2T cells [44] were injected into mammary fat pad of 6- to 10-week-old FVB/N mice and grown for 5 weeks. 1×10^6 4T1 cells [45] were injected into mammary fat pad of 6-week-old BALB/c mice and grown for 5 weeks.

Two-dimensional (2D) cultured MTflECad cells [46] were injected as a single-cell suspension in PBS at defined cell numbers into the ninth mammary gland of 7- to 10-week-old female BALB/c $Rag2^{-/-}$; common γ receptor$^{-/-}$ ($Rag2^{-/-}/\gamma c^{-/-}$; RG) mice [47].

Bone marrow transplantations

Bone marrow cells were extracted under sterile conditions from femurs and tibiae of donor C57BL/6-Tg(ACTB-EGFP) mice. After T cell depletion [48], 5×10^6 cells were injected in the tail vein of lethally irradiated (26550 cGy) 6-week-old RT2 mice, which were then killed for further analysis after 5–7 weeks of transplantation as reported elsewhere [29].

Anti-angiogenic treatments

RT2 or MMTV-PyMT mice were treated with either 100 mg/kg body weight PTK787/ZK222584 (PTK/ZK), dissolved in PEG-300 (Sigma, St. Louis, MO, USA) [49, 50] or with 100 µl/10 g body weight of PEG-300 alone (vehicle control) by daily oral administration for 5 days. For RT2 mice, the treatment started at the age of 8–9 or 12 weeks and for MMTV-PyMT mice started at 10 weeks. In addition, RT2 mice were treated for 10 days or 3 weeks starting at age 10 or 9 weeks, respectively. PTK/ZK was kindly provided by Novartis Pharma.

RT2 mice were treated with either 50 mg/kg body weight BIBF-1120 (nintedanib) dissolved in 0.5 % Natrosol (Sigma) [51] or 0.5 % Natrosol 100 µl/10 g body weight alone by daily oral administration for 5 days or 3 weeks starting at the age of 12 or 9 weeks, respectively. BIBF-1120 was kindly provided by Boehringer Ingelheim.

RT2 mice were treated with either 40 mg/kg body weight sunitinib malate (Sutent, S-8803, LC Laboratories, MA, USA) dissolved in sodium carboxymethylcellulose (Sigma) (CMC) solution (CMC: 0.5 %, NaCl 1.8 %, Tween 80 0.4 %, and benzyl alcohol 0.9 % in distilled water) or CMC 100 µl/10 g body weight alone by daily oral administration for 5 days or 3 weeks starting at the age of 12 or 9 weeks, respectively [52, 53].

Recombinant E1/E3-defective adenovirus expressing EGFP (Adenovirus-GFP) or soluble sFGFR2 (Adenovirus-trap-FGFR) was used as previously described [54, 55]. For the treatment of RT2 mice, 10^{10} virus particles/200 µl were injected into the tail vein once a week for 2 weeks, starting at the age of 10 weeks. In a combination regimen, RT2 mice were treated with either 100 mg/kg body weight PTK/ZK or PEG-300 100 µl/10 g body weight alone by daily oral administration for 10 days starting at the age of 10 weeks followed by 10^{10} virus particles/200 µl Adenovirus-trap-VEGFR2 or Adenovirus-GFP or Adenovirus-trap-FGFR tail vein injection once a week for 2 weeks.

Tumor-transplanted Py2T-FVB/N and 4T1-Balb/c mice were treated with either 50 mg/kg body weight BIBF-1120 or 0.5 % Natrosol 100 µl/10 g body weight alone by daily oral administration for 3 weeks starting when tumors reached measurable size.

Purification of PBMNCs from total blood

Total blood was drawn by heart puncture of euthanized mice or tail vein bleeding of living mice, diluted with one volume of PBS, and mixed. Two volumes of Hystopaque-10771 (Ficoll) (10771, Sigma) were added beneath diluted blood with a glass Pasteur pipette followed by centrifugation for 45 min at RT without brake at $650 \times g$. After the gradient separation, peripheral blood mononuclear cells (PBMNCs) were residing in a ring between plasma (top) and Ficoll (bottom). The ring with PBMNCs was collected, washed twice with 2 ml of FACS buffer (5 % FBS serum in PBS 1×), and the cells were counted.

Organ and tumor dissection

Spleen and lymph node were dissected from mice and kept in ice-cold PBS. The organs were minced, passed through a 70-μm cell strainer (352350, BD Bioscience, NJ, USA). Cells were collected (in PBS) and washed once in PBS. Erythrocyte lysis was performed with red blood cell (RBC) lysis buffer (NH_4Cl 1.5 M, $KHCO_3$ 0.1 M, EDTA 2.5 mM) for 10 min at RT and blocked with two volumes of PBS. Cells were then resuspended in FACS buffer and counted. Bone marrow was flushed from femurs and tibiae of mouse hind limbs with PBS, washed in PBS, and erythrocyte lysis was performed. Cells were resuspended in FACS buffer and counted.

Histopathological analysis

For histopathological analysis, the isolated organs were fixed in 4 % paraformaldehyde (Sigma) for 2 h at 4 °C and then incubated over night in 20 % sucrose in PBS at 4 °C and finally embedded in OCT (Tissue Tek, AGR1180, Agar Scientific, UK). Immunostainings were performed on 7-μm cryosections. After cutting, tissue sections were placed on slides, washed with PBS and then blocked for 60 min at RT or over night at 4 °C with 5 % goat serum in PBS (blocking buffer). Afterward, the sections were incubated for 60 min with rat anti-mouse CD31 (550274, BD Pharmingen, NJ, USA) diluted in blocking buffer, washed with PBS and incubated with the secondary antibody diluted in blocking buffer. After 30 min, sections were washed with PBS, nuclei were counterstained with DAPI (09542, Sigma), and slides were mounted with Mowiol (Sigma).

Flow cytometric analysis

Cells were washed in FACS buffer, Fc-blocked with a monoclonal antibody against mouse CD16/CD32 (dilution 1:100, Clone 93, 1-01302 BioLegend, CA, USA) for 10 min at RT and then stained for 30 min, at 4 °C in dark with conjugated antibodies of interest which were diluted in FACS buffer. Cells were then washed twice in FACS buffer and filtered through a filter with 40 μm pore size. Propidium Iodide (PI) (dilution 1:100, P4170, Sigma, St. Louis, MO, USA) or 6-diamidino-2-phenylindole (dilution 1:100, DAPI) was added to exclude dead cells immediately before analysis on a FACS Canto II (BD Bioscience, NJ, USA) or cell sorting on a FACS Aria II (BD Bioscience). Conjugate antibodies against: CD45 APC-Cy7 (dilution 1:500, clone 30-F11, 103116); IgM APC (dilution 1:100, clone EMM-1, 406509); IgD FITC (dilution 1:200, clone 11-26c.2α); CD93 PerCP-Cy5.5 (dilution 1:100, clone AA4.1, 136511); CD11b PerCP (dilution 1:200, clone M1/70, 101229); CD21 PerCP-Cy5.5 (dilution 1:1000 clone Avas 12α1, 123415); VEGFR2 PerCP (dilution 1:200, clone 89B3A5, 121915); VEGFR2 PE (dilution 1:200, clone 89B3A5, 121905); CD19 FITC (dilution 1:1000, clone 6D5, 115506) were purchased from BioLegend, CA. Tie2 (dilution 1:200, clone TEK4, 12-5987); CD31 PE-Cy7 (dilution 1:100, clone 390, 25-0311-81); CD31 FITC (dilution 1:200, clone 390, 11-0311-82); CD45 APC (dilution 1:800, clone 30-F11, 17-0451-88) were purchased from eBioscience. VEGFR2 PE (dilution 1:200, clone Ly-73, 555308), VEGFR1 PE (dilution 1:20, clone 141522, FAB4711P) and VEGFR1 APC (dilution 1:20, clone 141522, FAB4711A) were purchased from BD Pharmingen and R&D System, respectively. All the antibodies were diluted to stain 10^6 cells in a volume of 100 μl.

Real-time PCR

Total RNA was extracted from total tumors of 5 or 10 days PTK/ZK or PEG-300 treated RT2 mice using RNAeasy Mini Kit (74104, QIAGEN, Dusseldorf, Germany). First-strand cDNA was synthesized from 1 μg RNA using ImProm-II Reverse Transcriptase (M314C, Promega, Madison, WI, USA). Quantitative PCR for mouse *Vegfa*, *Vegfr1*, *Vegfr2*, *Vegfr3*, *Nrp1*, *Nrp2*, *Cd31*, *Fgf1*, *Fgf2* and *Hif1α* was done on a Step One Plus (Applied Biosystems-Life Technologies, Carlsbad, CA, USA) using a SYBR Green PCR MasterMix (Mesa Green qPCR MAsterMix Plus, Eurogentec, Liege, Belgium) and normalized versus mouse ribosomal protein 19 (mRPL19) transcript levels.

Gene expression profiling

PBMNCs were prepared by Hystopaque gradient from two different groups of 12-week-old RT2 mice and pooled within each group to get a biological duplicate. For subsequent isolation by flow cytometry, cells were first Fc-blocked with a monoclonal antibody against mouse CD16/CD32 and then stained with rat anti-mouse CD45 APC, rat anti-mouse VEGFR1 PE and rat anti-mouse CD31 FITC. $CD45^{dim}VEGFR1^{-}CD31^{low}$ cells were then isolated on a FACS Aria II. Total RNA was extracted from isolated cells using the Absolutely RNA Nanoprep Kit (Stratagene, CA, USA), amplified in two rounds (NuGen, CA, USA), IVT-labeled, fragmented and hybridized to GeneChip® Mouse 2.0 st microarray (Affymetrix, CA, USA).

Bioinformatics analysis

Gene expression profiles were background corrected and normalized using the RMA algorithm and subjected to quality control. The distribution of log2 expression values for each replicate as a mixture of two normal distributions

(non-expressed and expressed genes) was modeled using the mclust package, with $G = 2$ and modelNames = "V" [56]. Allowing for 5 % of false positives, a single cutoff for each replicate was defined. Genes with expression values above these thresholds in all replicates were classified as expressed in a given cell stage. The top 25 % of genes were selected based on their normalized absolute expression value. The resulting list of genes was subsequently subjected to GO term and pathway enrichment analysis using GeneCodis and Ingenuity Pathway Analysis (IPA), respectively.

HUVEC co-culture experiments

$CD45^{dim}VR1^{-}CD31^{low}IgM^{+}IgD^{-}$ and $CD45^{dim}VR1^{-}CD31^{high}$ cells were FACS-sorted from PBMNCs purified from fifteen 12-week-old RT2 mice. 10^5 sorted cells were mixed with 4×10^3 HUVECs and plated on top of growth factor-reduced Matrigel (356230, BD Bioscience) in μ-Slide Angiogenesis slides (81506, ibidi GmbH, Germany) in different media: EBM-2 basal (CC-3156, Lonza, Switzerland) or EGM-2 which is EBM-2 medium supplemented with growth factors (CC-3202, Lonza). Pictures were taken after 1.5, 2.5, 5, 6, and 17 h with a Leica DMI 4000 inverted microscope and analyzed using Image J (Angiogenesis analyzer plug-in).

Statistical analysis

All data are presented as means with standard errors of the mean (SEM) unless otherwise indicated. The Mann–Whitney *t* test (unilateral, unpaired, nonparametric test) was used for two-groups experiments and ANOVA for three-groups experiments. All statistical computations were done using GraphPad Prism v6.0c (GraphPad, La Jolla, CA, USA). Results were considered statistically significant when the *P* value was >0.05.

Results

The levels of $CD45^{dim}VEGFR1^{-}CD31^{low}$ cells are increased in tumor-bearing mice

In the initial experimental approaches, we have employed the RT2 transgenic mouse model of pancreatic β-cell carcinogenesis to screen for cell populations circulating at high levels in the peripheral blood of tumor-bearing mice [39]. In RT2 mice, the rat insulin promoter 1 (Rip1) drives expression of SV40 large T antigen (Tag) in insulin-producing pancreatic β-cells. Several tumor stages can be distinguished, including normal islets, β-cell hyperplasia, adenoma and carcinoma. Notably, hyperplastic islets can be classified into two types: non-angiogenic islets that do not affect co-cultured endothelial cells and angiogenic islets that are able to induce proliferation, migration, and tube formation of endothelial cells [57]. Based on these experiments, it has been proposed that soluble factors are involved in the onset of tumor angiogenesis (the angiogenic switch). In subsequent years, these mice have been used by us and others in a large number of studies for the functional characterization of pro-angiogenic factors (reviewed in [12]). To assess the generality and applicability of the findings, the MMTV-PyMT transgenic mouse model of metastatic breast cancer and syngeneic TRAMPC1-C57BL/6 mouse model of prostate cancer were also employed.

These mouse models were used for the identification of cells that correlate in their numbers in the peripheral blood with ongoing tumor angiogenesis (Supplementary Figure 1A). Peripheral blood was taken from these mice, and the levels of specific subpopulations of circulating cells in tumor-bearing mice as compared to healthy C57BL/6 mice were assessed by fluorescent staining of PBMNCs with combinations of antibodies defining certain subsets of EPCs, CECs and many other subtypes of bone marrow-derived mononuclear cells and subsequent flow cytometry analysis as detailed according to a previous report in Supplementary Figure 1B [8]. Since these surface markers are not exclusive for EPCs and CECs and are also expressed on other cell types, such as lymphocytes, myeloid cells and haematopoietic progenitor cells, we have used additional antibodies and combinations thereof to detect by flow cytometry particular cell populations in peripheral blood of mouse models of tumor angiogenesis in comparison with non-tumor-bearing mice (Supplementary Figure 1B).

By testing single markers and combinations of markers, four cell populations were identified whose levels correlated with tumor angiogenesis in 12-week-old RT2 mice (Fig. 1a–e), 10-week-old MMTV-PyMT mice and syngeneic TRAMPC1-C57BL/6 mice (Supplementary Figure 2). The four cell population levels were expressed as percentage of singlets and named on the basis of expression of the markers used for their identification: $CD45^{dim}VEGFR1^{-}$ ($CD45^{dim}VR1^{-}$), $CD45^{dim}VEGFR1^{-}CD31^{low}$ ($CD45^{dim}VR1^{-}CD31^{low}$), $VEGFR2^{+}TIE2^{+}VEGFR1^{-}$ ($VR2^{+}TIE2^{+}VR1^{-}$) and TEMs (TIE2-expressing monocytes, $TIE2^{+}CD45^{+}cKit^{-}CD11b^{+}CD31^{low}$) (Fig. 1b–e). Their levels were significantly higher in 12-week-old RT2 and in 10-week-old MMTV-PyMT mice in comparison with healthy C57BL/6 and FVB/N mice, respectively (Fig. 1b–e; Supplementary Figure 2A).

The levels of the $VR2^{+}TIE2^{+}VR1^{-}$ cell population in all mouse cancer models were found to be more variable and their correlation with tumor angiogenesis was less

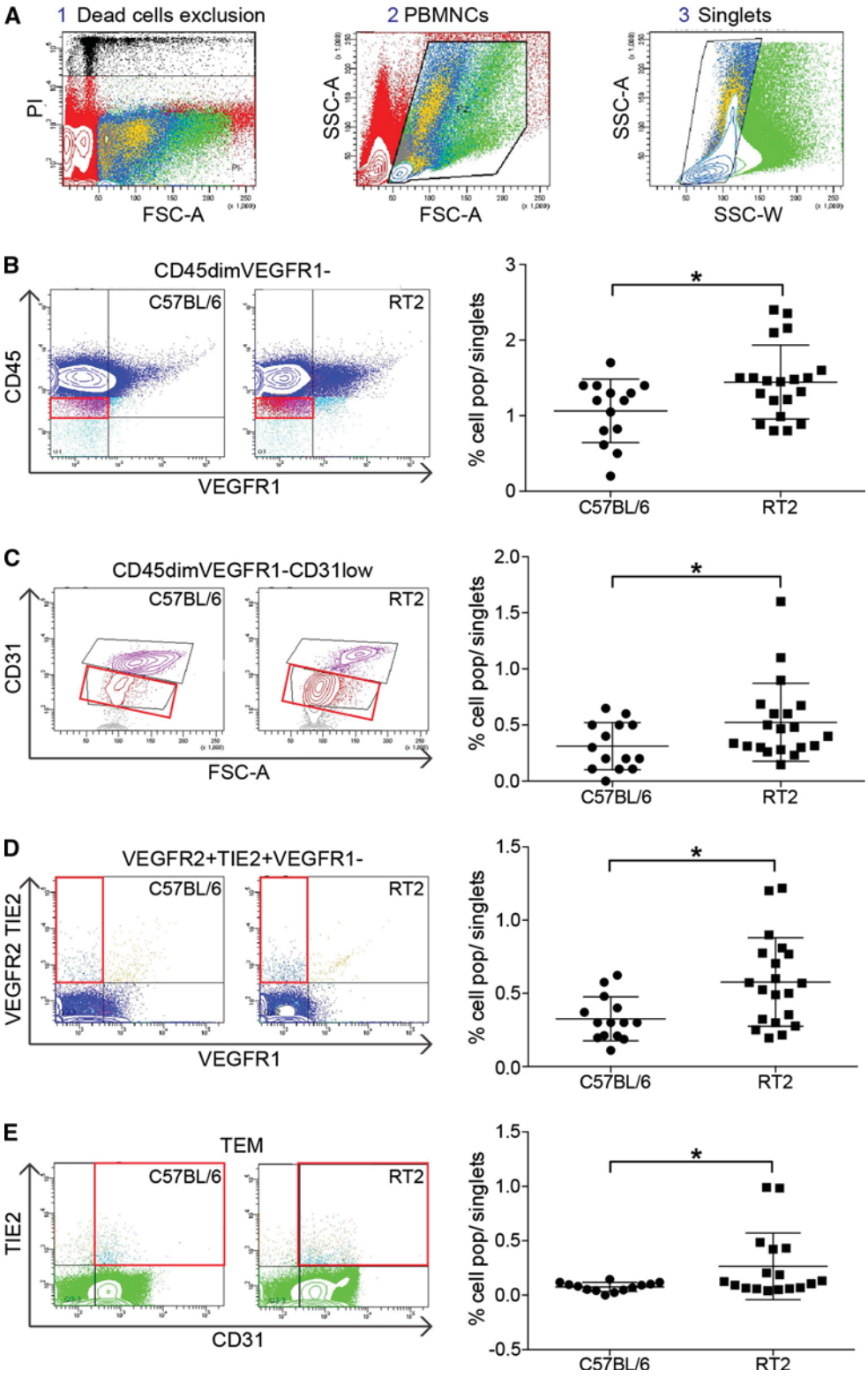

Fig. 1 Levels of four peripheral blood cell populations are increased in tumor-bearing RT2 mice. **a** Representative plots illustrate the flow cytometry strategy to identify peripheral blood mononuclear cells (PBMNCs) that are increased in levels in tumor-bearing transgenic RT2 mice as compared to non-transgenic control mice. The gates are: *1* dead cell exclusion by PI staining; *2* PBMNCs; *3* singlets. **b–e** Specific subpopulations that are increased in levels in tumor-bearing RT2 mice are identified by staining with specific cell surface markers and flow cytometry of singlets as described in (**a**). Shown are representative flow cytometry plots of $CD45^{dim}VR1^{-}$ (**b**), $CD45^{dim}VR1^{-}CD31^{low}$ (**c**), $TIE2^{+}VR2^{+}VR1^{-}$ (**d**) and TIE2-expression monocyte (TEM) (**e**) cell populations in healthy C57BL/6 and in 12-week-old RT2 mice. The *red squares* highlight the population of interest. Quantification of the levels of the cell population as percentages of living singlet PBMNCs is displayed in the graphs on the *right*. Mann–Whitney test: $*P < 0.05$. Each *dot* in the graphs represents an analyzed mouse. C57BL/6, $N = 13–14$; RT2, $N = 17–20$. Note that in (**d**) immunofluorescence staining with antibodies against TIE2 and VR2 was visualized with secondary antibodies labeled with the same fluorochrome (PE) to simultaneously detect TIE2 and VR2

robust; hence, they were excluded from further analyses. In addition, since TEMs have been well characterized in other studies [25, 58], we narrowed down our study to the previously uncharacterized $CD45^{dim}VR1^{-}$ and $CD45^{dim}VR1^{-}CD31^{low}$ cells. Their levels were found to be elevated also in the peripheral blood of syngeneic TRAMPC1-C57BL/6 mouse model compared to healthy control mice (Supplementary Figure 2B). Besides, the

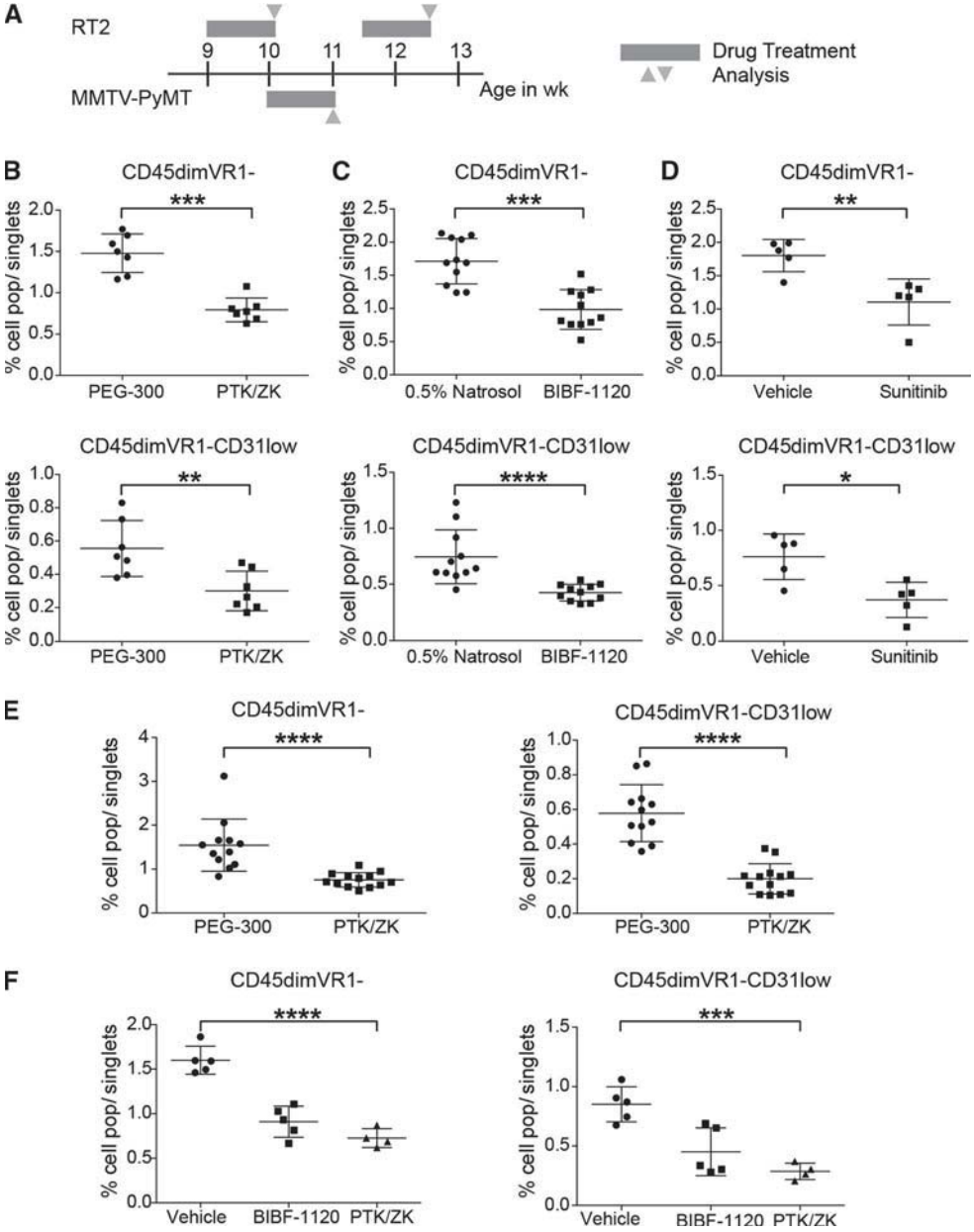

Fig. 2 Levels of $CD45^{dim}VR1^{-}$ and $CD45^{dim}VR1^{-}CD31^{low}$ cell populations are significantly reduced in peripheral blood of tumor mice upon short-term anti-angiogenic therapy. **a** Scheme of the anti-angiogenic regimen in RT2 and in MMTV-PyMT transgenic mice and subsequent flow cytometry analysis of their peripheral blood. $CD45^{dim}VR1^{-}$ and $CD45^{dim}VR1^{-}CD31^{low}$ cells were quantified by flow cytometry analysis in the peripheral blood of 11- to 12-week-old RT2 mice after 5 days of anti-angiogenic therapy with PTK/ZK (**b** PTK/ZK, $N = 7$; PEG-300, $N = 7$), BIBF-1120 (**c** BIBF-1120, $N = 11$; 0.5 % Natrosol, $N = 11$), or Sunitinib (**d** Sunitinib, $N = 5$; 0.5 % Natrosol, $N = 5$). Mann–Whitney test: $^{*}P < 0.05$; $^{**}P < 0.01$; $^{***}P < 0.005$; $^{****}P < 0.001$. **e** $CD45^{dim}VR1^{-}$ and $CD45^{dim}VR1^{-}CD31^{low}$ cells were quantified by flow cytometry analysis in the peripheral blood of MMTV-PyMT transgenic mice after 5 days of anti-angiogenic therapy with PTK/ZK (PTK/ZK, $N = 12$; PEG-300, $N = 13$). Mann–Whitney test: $^{****}P < 0.001$. **f** $CD45^{dim}VR1^{-}$ and $CD45^{dim}VR1^{-}CD31^{low}$ cells were quantified by flow cytometry analysis in the peripheral blood of 8- to 9-week-old RT2 mice after 5 days of BIBF-1120 ($N = 5$) or PTK/ZK ($N = 4$) treatments in comparison with 0.5 % Natrosol ($N = 5$). One-way Anova test: $^{***}P = 0.005$; $^{****}P < 0.001$

levels of $CD45^{dim}VR1^{-}$ and $CD45^{dim}VR1^{-}CD31^{low}$ cell populations were increased in 8- to 9-week-old RT2 mice, when the tumors were small and had only recently undergone an angiogenic switch, compared to healthy mice of the same age (Supplementary Figure 2C). These analyses suggest that $CD45^{dim}VR1^{-}$ and its subpopulation, $CD45^{dim}VR1^{-}CD31^{low}$, are consistently elevated during tumorigenesis in a variety of mouse cancer models. These populations thus may serve as surrogate markers to monitor early and late stage tumorigenesis in mouse models.

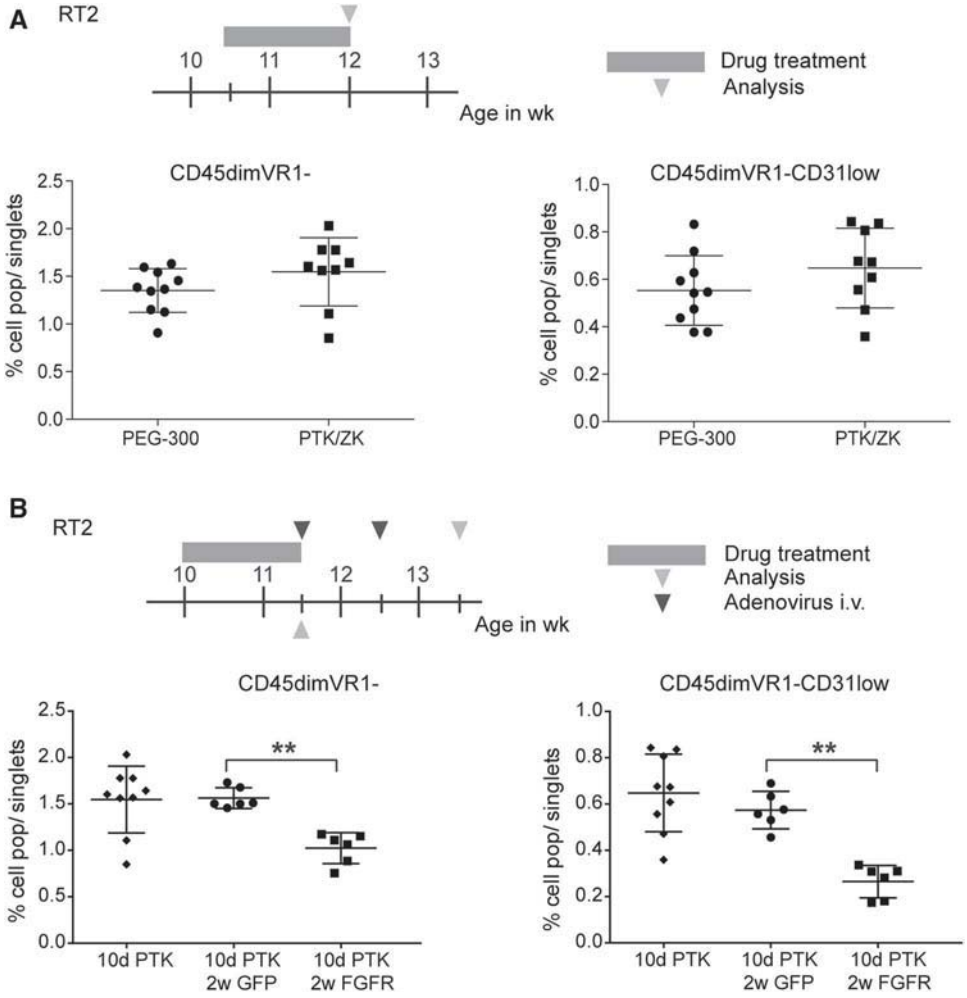

Fig. 3 Levels of $CD45^{dim}VR1^{-}CD31^{low}$ cells are preserved in the peripheral blood of RT2 mice after long-term anti-angiogenic treatment. **a** Schematic representation of 10-day PTK/ZK treatment in 10- to 11-week-old RT2 mice and subsequent flow cytometry analysis. Quantification of $CD45^{dim}VR1^{-}$ and $CD45^{dim}VR1^{-}CD31^{low}$ cell populations in the peripheral blood of these mice is shown below (PTK/ZK, $N = 9$; PEG-300, $N = 10$). **b** The scheme of the combinatorial treatment with PTK/ZK and adenovirus is shown on top. Quantification of $CD45^{dim}VR1^{-}$ and $CD45^{dim}VR1^{-}CD31^{low}$ cells in the peripheral blood of RT2 mice after 10 days of PTK/ZK treatment ($N = 9$), followed by 2 weeks of adenovirus treatment, is illustrated (GFP, $N = 6$; FGFR, $N = 6$). Mann–Whitney test: $^{**}P < 0.01$; $^{***}P < 0.005$

$CD45^{dim}VR1^{-}CD31^{low}$ cells decrease upon anti-angiogenic therapy

To investigate whether the cell populations described above are indeed good candidates as surrogate markers for tumor angiogenesis, tumor-bearing mice (12-week-old RT2 or 10-week-old MMTV-PyMT mice) were treated with different anti-angiogenic drugs, such as PTK/ZK (an inhibitor for all three VEGF receptors, all PDGF receptors, c-Kit and c-Fms), BIBF-1120 (nintedanib; inhibits all three VEGF receptors, PDGF receptors, all FGF receptors, FLT3 and members of the SRC-family [51]), and sunitinib malate (inhibits all PDGF receptors, VEGF receptor 1 and 2, c-Kit, FLT3 and RET; Fig. 2a). All the therapeutic regimens significantly reduced the tumor volume and microvessel density in tumor-bearing mice (Supplementary Figure 3A–C, data not shown). Peripheral blood was drawn from the treated mice, and the levels of the $CD45^{dim}VR1^{-}$ and $CD45^{dim}VR1^{-}CD31^{low}$ cell populations were assessed by flow cytometry (Fig. 2b–d). After 5 days of PTK/ZK (Fig. 2b), BIBF-1120 (Fig. 2c) or sunitinib (Fig. 2d) treatment, the levels of the two cell populations were significantly diminished as compared to placebo-treated mice and to levels found in peripheral blood of healthy mice (Fig. 1). Five days of PTK/ZK treatment in MMTV-PyMT mice also led to a significant decrease in the levels of $CD45^{dim}VR1^{-}$ and $CD45^{dim}VR1^{-}CD31^{low}$ cell populations (Fig. 2e). To assess whether a similar effect could also be observed for younger mice with early-stage cancer, a "short-term intervention trial" with PTK/ZK or BIBF-1120 was performed with 8- to 9-week-old RT2 mice. A 5-day treatment reduced tumor growth and microvessel densities (data not shown) and concomitantly decreased the cell populations in the peripheral blood of PTK/ZK-treated mice as compared to placebo-treated mice (Fig. 2f). These data indicate that anti-angiogenic therapy in RT2 mice and 10-week-old MMTV-PyMT mice leads to a repression of tumor angiogenesis and tumor growth [59] and concomitantly reduces the levels of $CD45^{dim}VR1^{-}$ and $CD45^{dim}VR1^{-}CD31^{low}$ cells circulating in the peripheral blood of tumor-bearing mice.

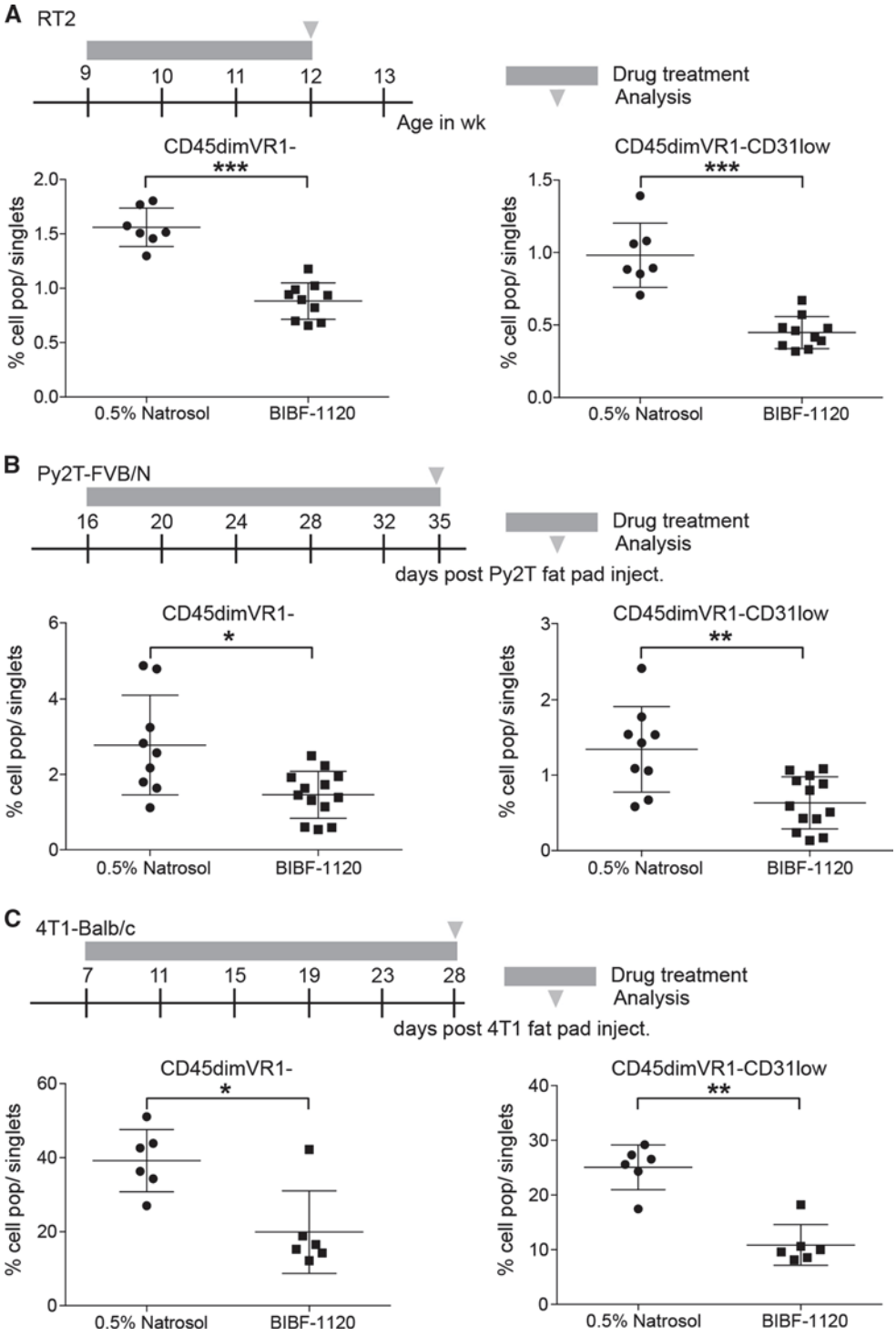

Fig. 4 Levels of $CD45^{dim}VR1^{-}$ and $CD45^{dim}VR1^{-}CD31^{low}$ cells are significantly reduced in peripheral blood of tumor-bearing mice upon 3 weeks of treatment with BIBF-1120 (nintedanib). **a–c** The scheme of the treatment and the quantification of $CD45^{dim}VR1^{-}$ and $CD45^{dim}VR1^{-}CD31^{low}$ cells by flow cytometry in peripheral blood of tumor-bearing mice treated with BIBF-1120 or vehicle control are shown. Quantification of $CD45^{dim}VR1^{-}$ and $CD45^{dim}VR1^{-}CD31^{low}$ cells is shown below. **a** RT2 transgenic mice treated with BIBF-1120 ($N = 10$) or 0.5 % Natrosol ($N = 7$). **b** FVB/N mice orthotopically transplanted with syngenic Py2T murine breast cancer cells treated with BIBF-1120 ($N = 12$) or Natrosol ($N = 9$). **c** Balb/c mice orthotopically transplanted with syngenic 4T1 murine breast cancer cells treated with BIBF-1120 ($N = 6$) or Natrosol ($N = 6$). Mann–Whitney test: $*P < 0.05$; $**P < 0.01$; $***P < 0.005$

The levels of $CD45^{dim}VR1^{-}CD31^{low}$ cells correlate with therapy resistance

In order to verify that $CD45^{dim}VR1^{-}$ and $CD45^{dim}VR1^{-}CD31^{low}$ cell populations could be further used as surrogate markers in a "long-term intervention trial," 10-week-old RT2 mice were treated for 10 days with PTK/ZK. Surprisingly, the levels of $CD45^{dim}VR1^{-}$ and $CD45^{dim}VR1^{-}CD31^{low}$ cells remained unaltered in the peripheral blood of RT2 mice after such longer treatment (Fig. 3a), although tumor growth and microvessel densities were efficiently reduced (Supplementary Figure 4A). Since it is well established that therapies targeting the VEGF signaling axis can lead to the upregulation of a panel of pro-

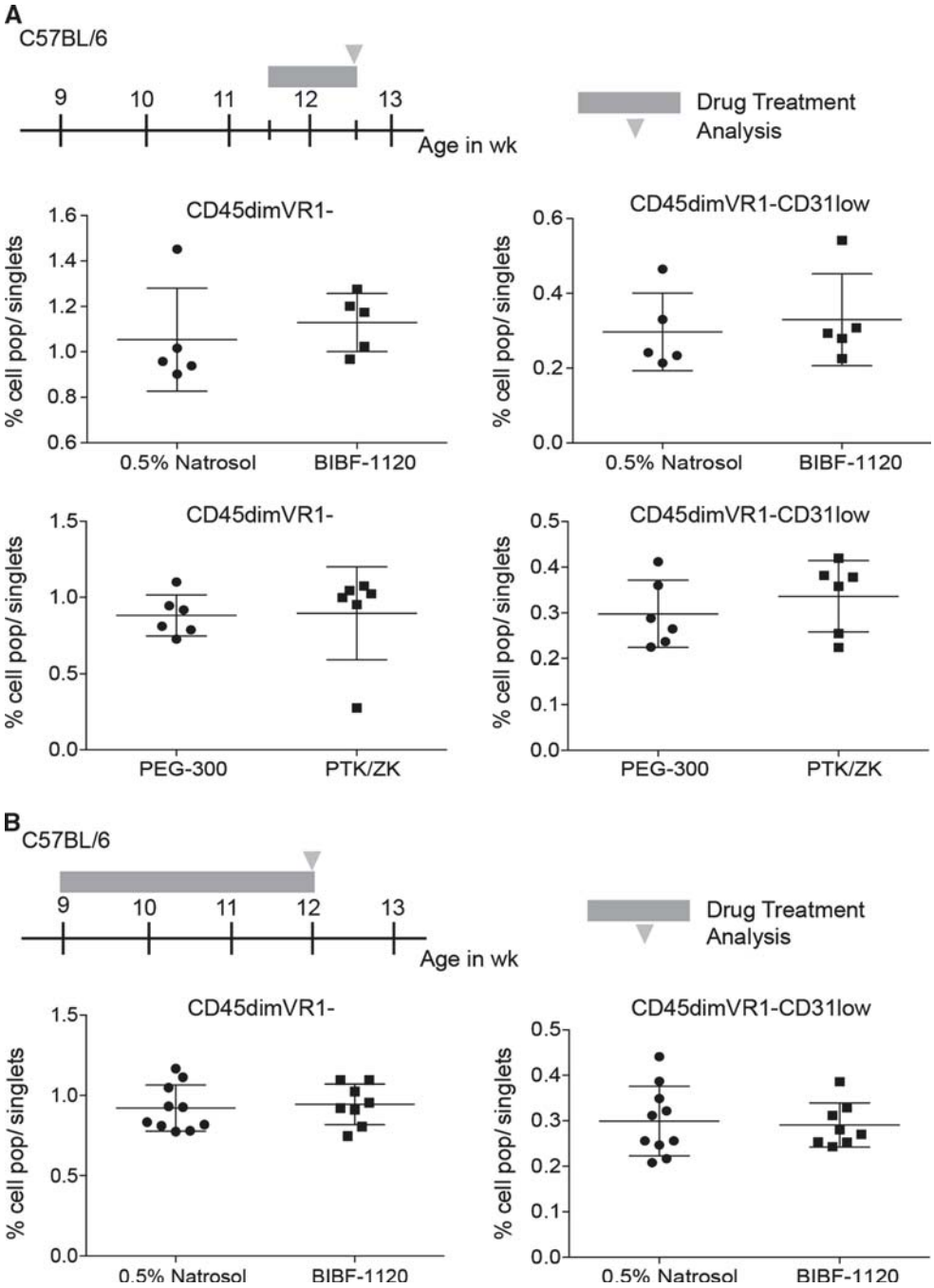

Fig. 5 Levels of $CD45^{dim}VR1^{-}$ and $CD45^{dim}VR1^{-}CD31^{low}$ in the peripheral blood of C57BL/6 mice are unaffected by anti-angiogenic therapy. Shown are the scheme of treatment and the quantification of $CD45^{dim}VR1^{-}$ and $CD45^{dim}VR1^{-}CD31^{low}$ by flow cytometry in peripheral blood of wild-type C57BL/6 mice **a** treated for 5 days with BIBF-1120 ($N = 5$), 0.5 % Natrosol ($N = 5$), PTK/ZK ($N = 6$) or PEG-300 ($N = 6$) or **b** treated for 3 weeks with BIBF-1120 ($N = 8$) or 0.5 % Natrosol ($N = 10$)

inflammatory and pro-angiogenic growth factors [34, 52, 53], we assessed whether the returning increase in the cell populations between a 5-day and a 10-day PTK/ZK treatment could reflect compensatory mechanisms overcoming the inhibitory activity of PTK/ZK, for example, by the activities of other angiogenic factors. Indeed, the levels of mRNAs encoding for *Fgf1*, *Fgf2* and *Vegf-a* were increased in tumors between 5- and 10-day treatment of RT2 mice with PTK/ZK (Supplemental Figure 4B). We thus assessed whether blocking FGF receptor signaling following PTK/ZK-mediated VEGF receptor inhibition could maintain the decrease in the levels of the surrogate cell populations. Previously, we have shown that recombinant adenovirus expressing a soluble FGF receptor trap (Adenovirus-trap-FGFR) can efficiently repress tumor angiogenesis by itself and in conjunction with anti-VEGF therapy [60]. Ten-week-old RT2 mice were first treated with PTK/ZK for 10 days and then intravenously injected with 10^{10} virus particles of Adenovirus-trap-FGFR for 2 weeks. $CD45^{dim}VR1^{-}$ and $CD45^{dim}VR1^{-}CD31^{low}$ cell

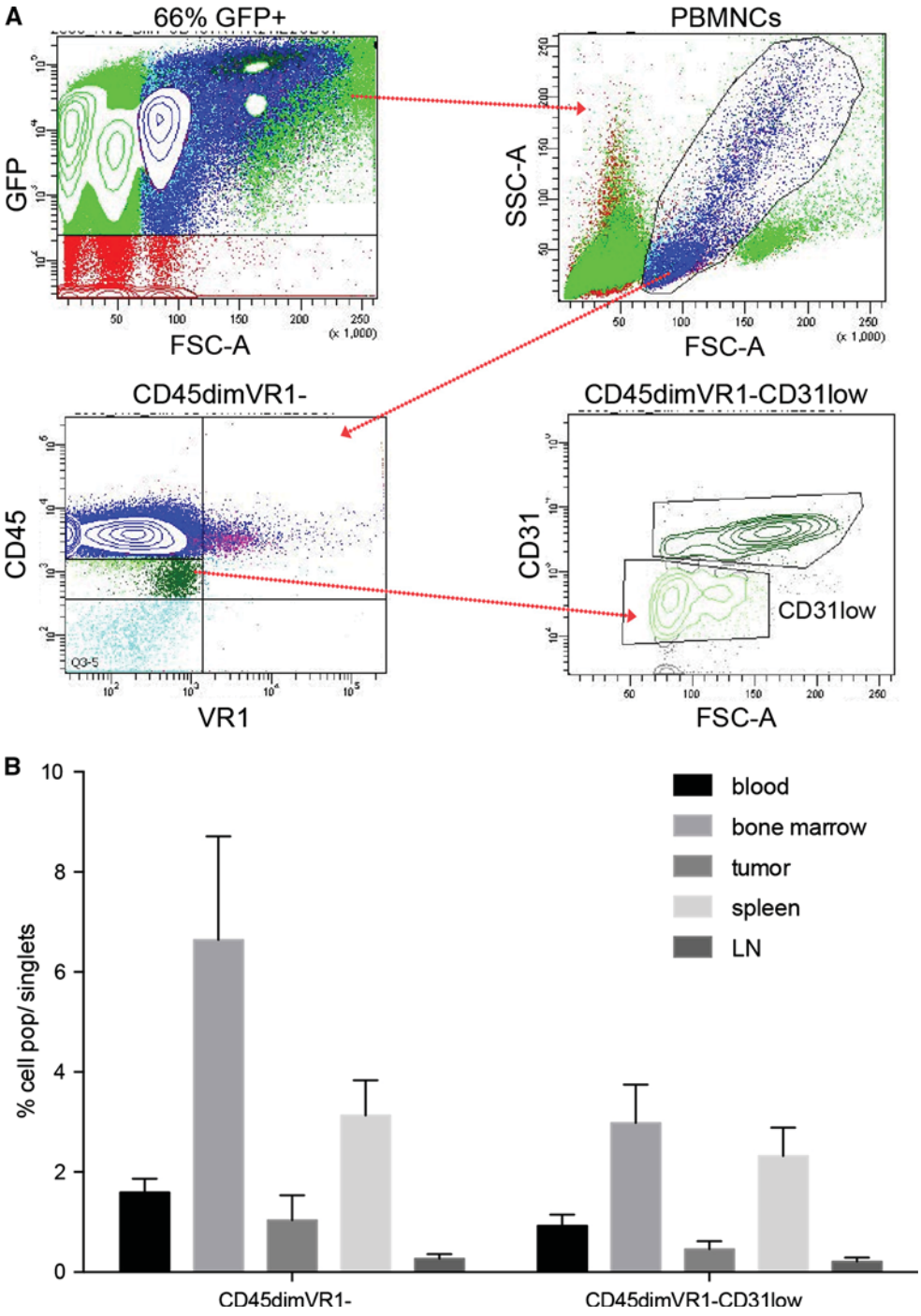

Fig. 6 $CD45^{dim}VR1^{-}CD31^{low}$ cells localize mainly in bone marrow, in blood and at lower levels in tumors. **a** $CD45^{dim}VR1^{-}CD31^{low}$ cells are bone marrow-derived as shown by flow cytometry analysis of blood from 12-week-old RT2 mice previously transplanted with bone marrow from C57BL/6-Tg(ACTB-EGFP) mice. **b** Quantification of the flow cytometry analysis of $CD45^{dim}VR1^{-}CD31^{low}$ cells in bone marrow, blood, spleen, lymph nodes (LN) and tumors of RT2 mice (number of experiments = 3; number of mice = 6)

population levels were high after 10 days of PTK/ZK treatment; however, they were abated significantly upon the subsequent blockade of FGF signaling (Fig. 3b). Intra-tumoral vessel density was also diminished compared to control mice; however, tumor volumes were non significantly increased upon Adenovirus-trap-FGFR treatment, an observation that may involve non-angiogenesis-related effects on tumor growth and needs further investigations (Supplementary Figure 4C).

To validate these findings, RT2 transgenic mice and Py2T-FVB/N and 4T1-BALB/c tumor-bearing mice were treated for 3 weeks with BIBF-1120 (nintedanib; Fig. 4a–c). The $CD45^{dim}VR1^{-}$ and $CD45^{dim}VR1^{-}CD31^{low}$ cell populations in the peripheral blood of the various BIBF-1120-treated mouse cancer models were significantly decreased compared to vehicle-treated mice. As expected, tumor growth and intra-tumoral vessels were substantially reduced by treatment with BIBF-1120 (data not shown).

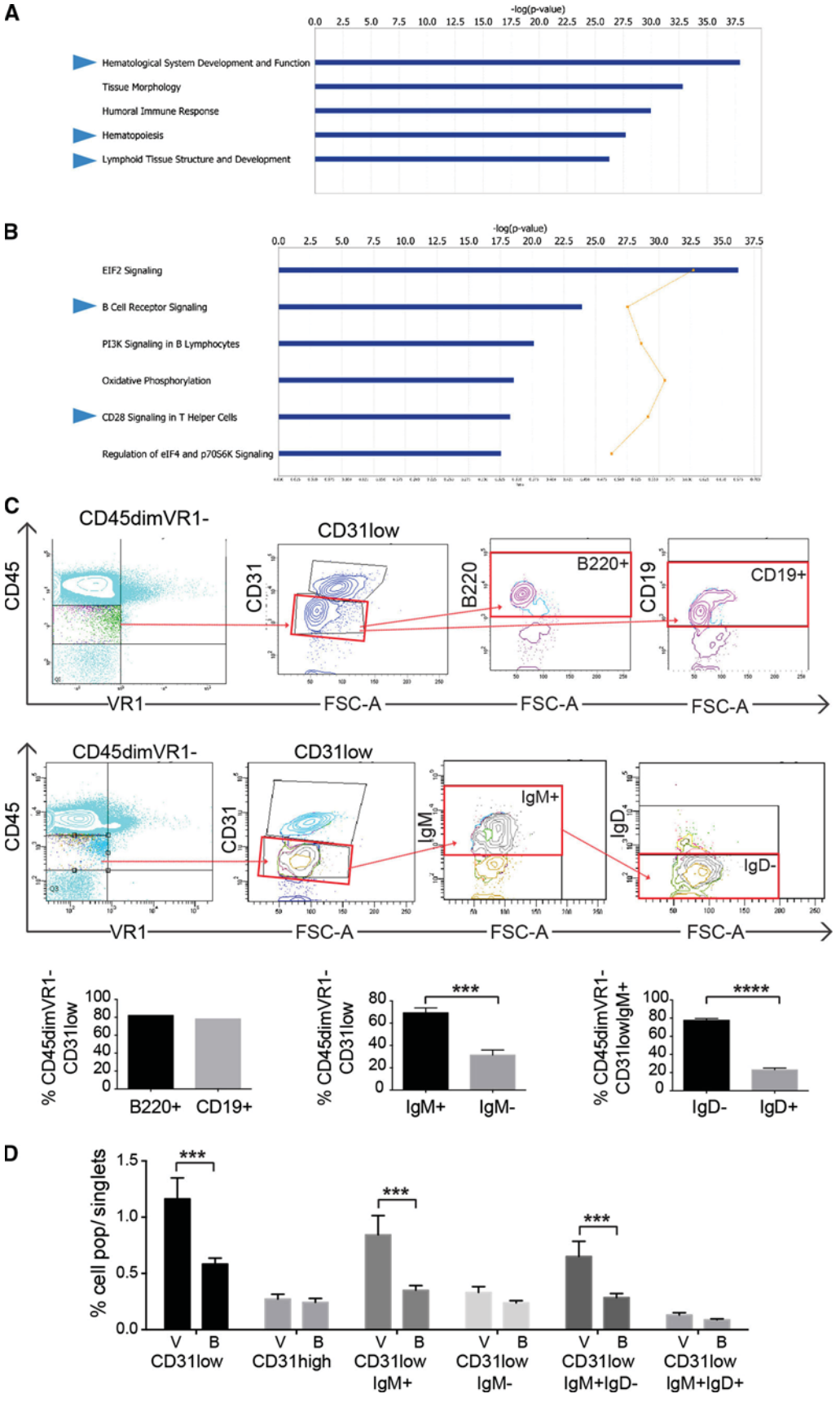

◀**Fig. 7** Gene expression profiling and flow cytometry classify $CD45^{dim}VR1^{-}CD31^{low}$ cells as immature B cells. **a**, **b** Gene expression profiling of $CD45^{dim}VR1^{-}CD31^{low}$ cells by Affymetrix Chip analysis and subsequent IPA software analysis reveals enriched physiological pathways. The top five enriched functions within the physiological system development and function category (**a**) and signaling pathways category (**b**) are shown. Highest coverage was observed within the B cell receptor signaling and antigen presentation pathways. **c** Flow cytometry analysis of PBMNCs from 12-week-old RT2 mice for B220, CD19, IgM and IgD expression in the $CD45^{dim}VR1^{-}CD31^{low}$ cell population. The percentages of the $CD45^{dim}VR1^{-}CD31^{low}$ cell population positive for B220 (82.9 %) and CD19 (76.7 %), and positive (69.324 %; 21 %) or negative (31.292 %; 79 %; $N = 10$) for IgM and for IgD are shown below. **d** Quantification of immature B cell markers in 12-week RT2 mice treated with BIBF-1120 (**b** $N = 10$) or 0.5 % Natrosol (V, $N = 10$) for 5 days. CD31low = $CD45^{dim}VR1^{-}CD31^{low}$; CD31high = $CD45^{dim}VR1^{-}CD31^{high}$; CD31lowIgM + = $CD45^{dim}VR1^{-}CD31^{low}IgM^{+}$; CD31lowIgM^{-} = $CD45^{dim}VR1^{-}CD31^{low}IgM^{-}$; CD31lowIgM^{+}IgD^{-} = $CD45^{dim}VR1^{-}CD31^{low}IgM^{+}IgD^{-}$. Mann–Whitney test: ***$P < 0.005$; ****$P < 0.001$. N = number of mice; V = vehicle; B = BIBF-1120

Notably, the lower levels of $CD45^{dim}VR1^{-}$ and $CD45^{dim}VR1^{-}CD31^{low}$ cells in the peripheral blood of healthy mice were not altered upon short-term PZK/ZK treatment or short- or long-term treatment with BIBF-1120 (Fig. 5a, b), and thus the drugs were not directly targeting the cell populations as such. Also, the extensive microvasculature present in normal islets of Langerhans was not affected by either treatment, and hence the drugs were targeting exclusively active pathological angiogenesis (Supplementary Figure 5).

$CD45^{dim}VR1^{-}CD31^{low}$ cells represent bone marrow-derived immature B cells

To determine the cell lineage of the $CD45^{dim}VR1^{-}CD31^{low}$ cell population, lethally irradiated RT2 mice were transplanted with bone marrow isolated from actin-GFP transgenic mice [29, 42]. Flow cytometry analysis of peripheral blood showed an efficient hematopoietic reconstitution of the hematopoietic system with about 70 % chimerism in the transplanted mice and demonstrated that the $CD45^{dim}VR1^{-}$ and $CD45^{dim}VR1^{-}CD31^{low}$ cell populations were GFP-positive, indicating that they originated from bone marrow (Fig. 6a). $CD45^{dim}VR1^{-}$ and $CD45^{dim}VR1^{-}CD31^{low}$ cells not only circulated in peripheral blood, but were also found in spleen, lymph node and, with lower incidence, in tumors of RT2 mice (Fig. 6b). Thus, $CD45^{dim}VR1^{-}$ and $CD45^{dim}VR1^{-}CD31^{low}$ are PBMNCs that are mobilized from the bone marrow in response to angiogenic stimuli generated by tumor cells or cells of the tumor stroma in the RT2 transgenic mouse model.

To determine the cell lineage identity of the potential surrogate marker cell population, $CD45^{dim}VR1^{-}CD31^{low}$ cells were isolated by flow cytometry sorting from peripheral blood of RT2 mice and subjected to gene expression profiling by Affymetrix Chip analysis. R and Ingenuity Pathway Analysis (IPA) pinpointed that many genes of the $CD45^{dim}VR1^{-}CD31^{low}$ transcriptome were clustered in five classes within the Physiological System Development and Function categories in IPA (Fig. 7a; Online Resource 1, Online Resource 2). Among those classes were hematopoiesis, lymphoid tissue structure and hematological system development and function. Furthermore, in the canonical pathways as defined by IPA, a high degree of coverage of pathway gene members was found to belong to B cell receptor signaling (Fig. 7b).

B cell development is initiated in the fetal liver before birth and in the bone marrow in adults, yet subsequent functional maturation occurs in secondary lymphoid organs. B cells that have exited the bone marrow migrate to the spleen where they undergo further maturation via transitional stages identified by the expression of markers such as CD21 (CD23 in the mouse) and eventually reaching the final maturation as follicular B cells. T cell-dependent immune responses induce additional germinal center (GC) maturation in secondary lymphoid organs. B cells in peripheral compartments may also belong to more specialized B cell subsets including $CD5^{+}$ B1 cells, which have a role in tumor angiogenesis [61], or marginal zone (MZ) B cells. Germinal center maturation of B cells leads to the generation of memory B cells and the development of antibody secreting plasma cells (Supplementary Figure 6A) [62–65].

IPA analysis also generated a list of genes specifically localized in the plasma membrane or in the extracellular space (Online Resource 1), and subsequent flow cytometry analyses confirmed the expression of cell surface markers for immature B cells on the $CD45^{dim}VR1^{-}CD31^{low}$ cell population. The $CD45^{dim}VR1^{-}CD31^{low}$ cell population circulating in the blood was 70–80 % positive for B220, IgM and CD19, and about 70–80 % of $CD45^{dim}VR1^{-}CD31^{low}IgM^{+}$ cells were negative for IgD, identifying them as an immature B cell population (Fig. 7c, Supplementary Figure 6A). Immature B cells lack the expression of CD21/CD23 and, indeed, $CD45^{dim}VR1^{-}CD31^{low}$ cells were about 90 % negative for CD21 and CD23 (Supplementary Figure 6B). Furthermore, $CD45^{dim}VR1^{-}CD31^{low}IgM^{+}IgD^{-}$ cells were about 70–80 % CD21 negative (Supplementary Figure 6C), confirming their immature phenotype. In addition, they did not express CD5 (data not shown), indicating they did not represent a specialized B cell subset named B1 cells [65].

To further validate $CD45^{dim}VR1^{-}CD31^{low}IgM^{+}IgD^{-}$ immature B cells as potential surrogate markers, 12-week-old RT2 mice were treated with BIBF-1120 (nintedanib) for 5 days. In comparison with placebo-treated RT2 mice, exclusively the levels of $CD45^{dim}VR1^{-}CD31^{low}$,

$CD45^{dim}VR1^{-}CD31^{low}IgM^{+}$ and $CD45^{dim}VR1^{-}CD31^{low}IgM^{+}IgD^{-}$ cell subpopulations were found reduced in BIBF-1120-treated RT2 mice (Fig. 7d). Moreover, immunofluorescence microscopy analysis of tumors from 12-week-old RT2 mice (Supplementary Figure 7A) as well as flow cytometry analyses (Supplementary Figure 7B) showed that immature B cells were sporadically infiltrating tumors of 12-week-old RT2 mice. In addition, since immature B cells mobilize from bone marrow to spleen to complete their maturation, the presence of our population of interest in bone marrow and in spleen validated their immature phenotype.

Immature B cells promote endothelial cell to form cord-like structures

In order to obtain a first glimpse into a potential functional contribution of $CD45^{dim}VR1^{-}CD31^{low}IgM^{+}IgD^{-}$ immature B cells to tumor angiogenesis, human umbilical venous endothelial cells (HUVEC) were co-cultured with $CD45^{dim}VR1^{-}CD31^{low}IgM^{+}IgD^{-}$ immature B cells in three-dimensional Matrigel growth conditions. Under these growth conditions, HUVEC form cord-like structures in the presence of growth-stimulating EBM2 culture medium, but not in the presence of basal medium only. Notably, in the presence of $CD45^{dim}VR1^{-}CD31^{low}IgM^{+}IgD^{-}$, HUVEC cells also formed differentiated cord-like structures comparable to EBM2 medium (Fig. 8). These results raise the possibility that immature B cells, mobilized by ongoing tumor angiogenesis and repressed in numbers by anti-angiogenic therapy, may not only serve as surrogate marker for tumor angiogenesis but may also indirectly support tumor angiogenesis. However, the latter notion requires further validation in mouse models in vivo.

Discussion

The development of predictive biomarkers for anti-angiogenic therapies is urgently needed to select those patients who most likely will benefit from anti-angiogenic therapy and to prevent unnecessary loss of time and toxicity in therapy-resistant patients. Despite numerous attempts, thus far no validated biomarker to monitor ongoing tumor angiogenesis is available for routine clinical use. For example, elevated levels of VEGF in tumors are known to correlate with advanced clinical stage and poor prognosis; however, analyses of VEGF expression levels in tissue samples of breast and colorectal cancer treated with bevacizumab do not predict response to anti-angiogenic therapy [66]. An example of a functional parameter used as biomarker is tumor microvessel density. It reflects the amount of vascularization in tumors and, thus, is a good prognostic factor, yet it has failed as a predictive biomarker for treatment response in clinical settings. As cellular biomarkers, the numbers of CECs and EPCs in the blood correlate with angiogenesis and tumor progression, and their increased levels return to normal following anti-angiogenic treatments [67]. However, in certain type of cancers, these numbers have not correlated with the efficacy of anti-angiogenic therapies and, therefore, reproducibility and standardization of these approaches are challenging if not limiting for routine clinical use [68]. It is thus critical to identify a reliable prognostic and predictive biomarker for tumor angiogenesis.

Here, we report the identification of $CD45^{dim}VR1^{-}CD31^{low}IgM^{+}IgD^{-}$ bone marrow-derived immature B cells circulating in the peripheral blood of tumor-bearing mice as potentially useful surrogate marker for tumor angiogenesis. First, this cell population has been found increased in the peripheral blood of transgenic RT2 and MMTV-PyMT models of insulinoma and breast cancer, respectively, and of syngeneic prostate and breast transplantation models of cancer. Second, the levels of $CD45^{dim}VR1^{-}CD31^{low}IgM^{+}IgD^{-}$ immature B cells in peripheral blood were reduced exclusively in tumor-bearing mice after anti-angiogenic treatments blocking VEGF, PDGF and/or FGF signaling pathways, indicating that these cells could be a good predictive biomarker of anti-angiogenic therapy response. The generality of the results raises the possibility that $CD45^{dim}VR1^{-}CD31^{low}IgM^{+}IgD^{-}$ cells may serve as surrogate markers for the status of tumor angiogenesis in many different mouse models of cancer and with varying anti-angiogenic regimen.

However, upon variation of the duration of different anti-angiogenic therapies, we observed that the specific targeting of only one angiogenic signaling pathway resulted only in a short-term reduction in the surrogate marker cell population. For example, interfering with VEGF signaling alone by PTK/ZK or a neutralizing antibody to VEGF receptor 2 (DC101; data not shown) failed to reduce the cell population levels in peripheral blood of RT2 mice after long-term treatment, despite a substantial reduction in microvessel densities and tumor growth. Specifically, we observed a reduction in the $CD45^{dim}VR1^{-}CD31^{low}$ cell population in peripheral blood of RT2 mice after 5 days but not after 10 days of PTK/ZK treatment. We suspect that the re-establishment of higher levels of $CD45^{dim}VR1^{-}CD31^{low}$ cells may indicate the development of resistance against the mono-target therapies. In fact, it has been previously reported that already 1 week of treatment of RT2 mice with DC101 leads to tumor hypoxia and the subsequent upregulated expression of FGF, VEGF and Ang2 resulting in more vascularized and invasive tumors [52, 53]. We found that the 10-day treatment of RT2

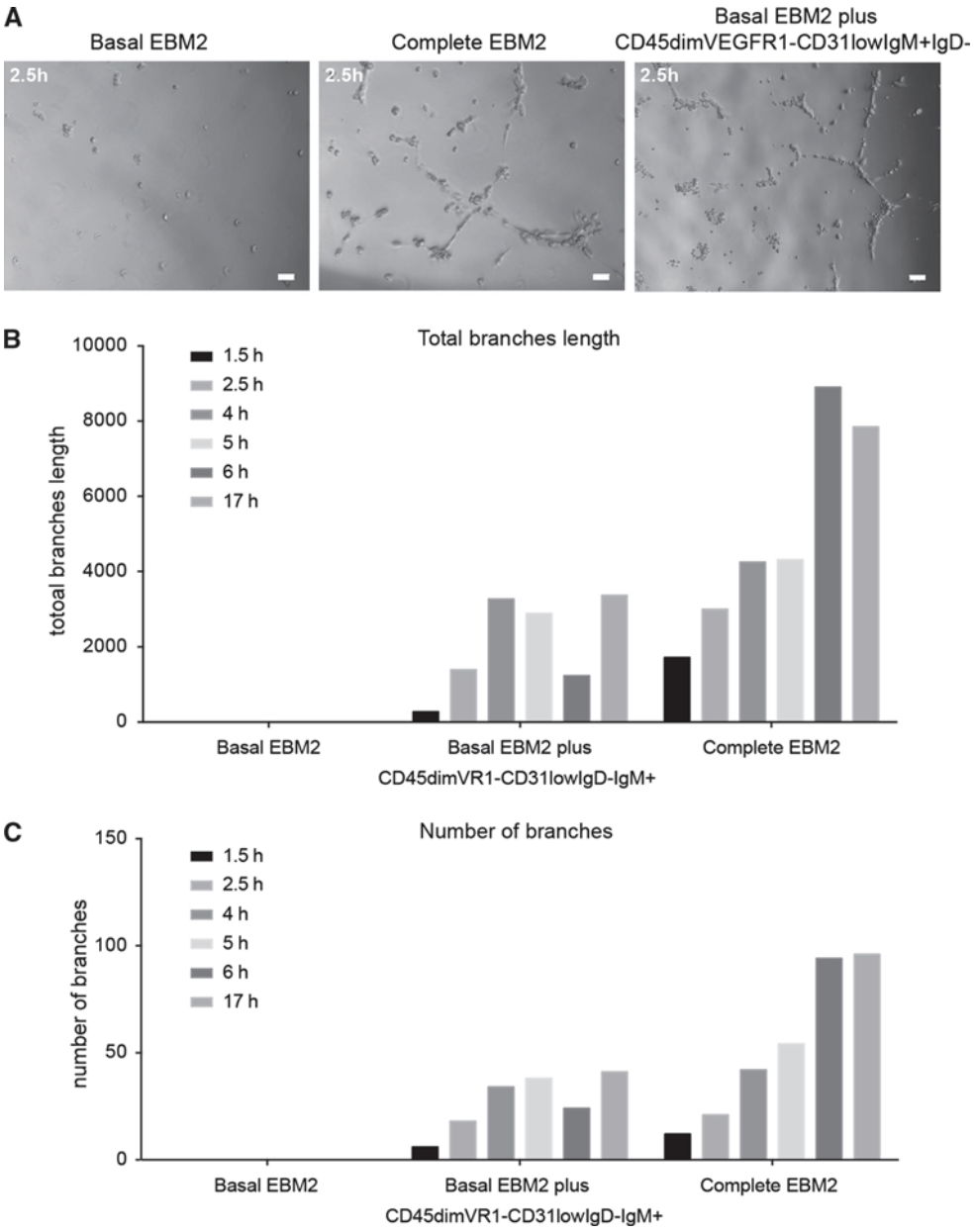

Fig. 8 $CD45^{dim}VR1^{-}CD31^{low}$ immature B cells are able to induce endothelial cells cord formation in vitro. **a** Representative images of HUVEC cells co-cultured in Matrigel with $CD45^{dim}VR1^{-}CD31^{low}$ immature B cells sorted from peripheral blood of RT2 mice are shown: HUVEC cells cultured in basal EBM2 medium (EBM2 medium minus growth factors; *left*), HUVEC cells cultured in complete EBM2 medium (EBM2 plus growth factors; *center*), and HUVEC cells co-cultured with $CD45^{dim}VR1^{-}CD31^{low}$ immature B cells in basal EBM2 medium (*right*). **b**, **c** Quantification of the length (**b**) and number (**c**) of branches formed after 1.5, 2.5, 4, 5, 6 and 17 h of culture, as quantified using the Angiogenesis tool in ImageJ software. *Scale bars* 100 μm

mice with PTK/ZK also promoted the expression of the angiogenic factors FGF1 and FGF2, and we treated the mice with Adenovirus-trap-FGFR-trap for 2 weeks and found a further decrease in microvessel densities as well as a reduction in the levels of $CD45^{dim}VR1^{-}CD31^{low}$ cells in comparison with RT2 mice treated with PTK/ZK for 10 days alone. Thus, the augmented levels of $CD45^{dim}VR1^{-}CD31^{low}$ cells in RT2 mice treated for 10 days could be a first sign of evasive resistance to this drug mainly targeting VEGF receptors only, supporting the hypothesis that this cell population could be a good predictive marker of anti-angiogenic therapy response.

In contrast to the mono-target therapies, the levels of $CD45^{dim}VR1^{-}CD31^{low}$ cells remained reduced upon long-term treatment of RT2 mice with the multi-kinase inhibitor BIBF-1120 (nintedanib), suggesting that it exerts a highly effective and sustainable anti-angiogenic activity. Thus, as speculated before, several pro-angiogenic signals triggered by the tumor microenvironment can possibly mobilize $CD45^{dim}VR1^{-}CD31^{low}$ immature B cells from the bone marrow. Indeed, gene expression profiling analysis of $CD45^{dim}VR1^{-}CD31^{low}$ cells (Online Resource 1) revealed the expression of several growth factor receptors, such as FGFR1, IGFR1, INSR and EGFR and pro-angiogenic factors, such as VEGF, PDGFs, FGFs, ILs, insulin and EGF. Notably, $CD45^{dim}VR1^{-}CD31^{low}$ cells were never found increased in tumor-bearing immune-deficient mice (Supplementary Figure 8, [47]), indicating that the

surrogate marker cell population not only depends on the mobilization by active tumor angiogenesis but also on a functional immune system. Finally, co-culture experiments with HUVECs indicate that $CD45^{dim}VR1^{-}CD31^{low}$ cells support the differentiation of endothelial cells in vitro. Previously, the Hanahan and the Coussens groups have shown that tumor angiogenesis was not affected in Rip1-Tag2 and PyMT mice that have been depleted of B cells [52, 69]. Thus, the nature of the possible pro-angiogenic activity of our cell population of interest, most likely exerted by secreted pro-angiogenic factors, remains to be further investigated, notably in mouse models in vivo.

Gene expression profiling and flow cytometry analysis classified the $CD45^{dim}VR1^{-}CD31^{low}$ cell population as immature B cells, positive for the B cell lineage markers B220, CD19 and IgM and negative for IgD, CD23 and CD21. Although the immature B cells were found to be bone marrow-derived and circulating in the blood, they were also present in spleen and at very low levels in lymph nodes and in tumors. The low percentage detected in lymph nodes of RT2 mice support the findings that the surrogate marker cell population indeed exhibits an immature phenotype, since only mature B cells are known to localize to lymph nodes [70]. Furthermore, the localization in spleen indicated the possibility that the cell population could complete its development to mature B cells. However, further studies are warranted to address whether the $CD45^{dim}VR1^{-}CD31^{low}$ cells are able to complete maturation to B cells and what their functional role in tumor angiogenesis in vivo could be.

Indeed, several reports have described the dual role of immune system in tumor progression and angiogenesis [11, 71]. The majority of the studies have focused on tumor-infiltrating cells of the immune system and are crucial mediators of cancer initiation and progression. For instance, B cells have been found in aggregates with other immune cells in several human cancer types [72]. Although various studies have demonstrated the beneficial effects of B cells tumor infiltration on anticancer immunity [73], it has been reported that B cells are required for de novo carcinogenesis in mouse models of skin cancer [74] and that B cells producing TNFα are important in papilloma development [75]. Yang et al. [76] have shown that B cells with activated STAT3 signaling produce pro-angiogenic factors resulting in increased angiogenesis and accelerated tumor progression. Furthermore, $B220^{low}IgM^{high}CD11b^{+}$ (so-called B1 cells [77]) have been found to drive M2-like polarization of macrophages and to promote the growth of transplanted B16 melanoma [61]. Thus, the immature B cell surrogate marker population we have identified may exert an indirect role in tumor angiogenesis, comparable to the B1 cell subpopulation, which they closely resemble according to their B cell marker expression.

Increased levels of CECs, EPCs and bone marrow-derived cells have been reported not only in the presence of active tumor angiogenesis, but also in a broad spectrum of vascular disease with aberrantly increased angiogenesis, such as damage to the vessel wall caused by mechanical stress, ischemia, infection or autoimmune reactions [38, 78–80]. To assess whether the immature B cells population is also increased in mice that are tumor free but exhibit increased angiogenesis in a normal organ, we have employed the Rip1VEGF-E transgenic mouse model of upregulated angiogenesis in normal islets of Langerhans (Supplementary Figure 9A). VEGF-E_{D1701} is a homologue of VEGF-A and a potent angiogenic factor binding exclusively to VEGFR-2 and Nrp1 and, thus, inducing endothelial cell proliferation, migration and sprouting [81, 82]. Rip1VEGF-E mice are characterized by increased endothelial cell proliferation in the islets of Langerhans of the pancreas, resulting in the formation of haemangioma-like structures (Fagiani et al., unpublished). We did not detect a significant increase in $CD45^{dim}VR1^{-}CD31^{low}$ immature B cells in the peripheral blood of these mice as compared to non-transgenic control mice (Supplementary Figure 9B), indicating that the levels of the surrogate marker cell populations are only increased by tumor-associated angiogenesis.

In summary, we have identified an immature B cell population to represent a robust and general surrogate marker to monitor active tumor angiogenesis and the efficacy of anti-angiogenic therapy in diverse mouse models of cancer. These surrogate marker cells are readily quantifiable by flow cytometry in the peripheral blood of mice, and the markers used to define them are conserved in humans [83]. Hence, it will be interesting to monitor the levels of these or comparable cells in patients that are undergoing anti-angiogenic therapy, an effort that will require specifically designed clinical studies.

Acknowledgments We are grateful to H. Antoniadis, U. Schmieder and R. Jost for the technical support. The authors thank M. Saxena for critical comments on the manuscript, T. Barthlott and P. Demougin (University of Basel) for expertise in cell sorting and Affymetrix GeneChip analysis, A.G. Rolink (University of Basel) for expertise on B cell development, and R. Goosen (University of Basel) for gene expression profiling analysis. This work was supported by a Collaborative Cancer Research Project of the Swiss Cancer League (CCRP OCS-01812-12-2005) and a MD-PhD fellowship to R.B. by the Swiss National Science Foundation.

Conflict of interest The authors declare no conflict of interest.

References

1. Folkman J (1971) Tumor angiogenesis: therapeutic implications. N Engl J Med 285(21):1182–1186. doi:10.1056/NEJM197111182852108

2. Carmeliet P (2005) Angiogenesis in life, disease and medicine. Nature 438(7070):932–936. doi:10.1038/nature04478
3. Folkman J (2007) Angiogenesis: an organizing principle for drug discovery? Nat Rev Drug Discov 6(4):273–286. doi:10.1038/nrd2115
4. Gacche RN, Meshram RJ (2014) Angiogenic factors as potential drug target: efficacy and limitations of anti-angiogenic therapy. Biochim Biophys Acta 1846(1):161–179. doi:10.1016/j.bbcan.2014.05.002
5. Ebos JM, Lee CR, Cruz-Munoz W, Bjarnason GA, Christensen JG, Kerbel RS (2009) Accelerated metastasis after short-term treatment with a potent inhibitor of tumor angiogenesis. Cancer Cell 15(3):232–239. doi:10.1016/j.ccr.2009.01.021
6. Leung DW, Cachianes G, Kuang WJ, Goeddel DV, Ferrara N (1989) Vascular endothelial growth factor is a secreted angiogenic mitogen. Science 246(4935):1306–1309
7. Senger DR, Galli SJ, Dvorak AM, Perruzzi CA, Harvey VS, Dvorak HF (1983) Tumor cells secrete a vascular permeability factor that promotes accumulation of ascites fluid. Science 219(4587):983–985
8. Bertolini F, Shaked Y, Mancuso P, Kerbel RS (2006) The multifaceted circulating endothelial cell in cancer: towards marker and target identification. Nat Rev Cancer 6(11):835–845. doi:10.1038/nrc1971
9. Kerbel RS (2008) Tumor angiogenesis. N Engl J Med 358(19):2039–2049. doi:10.1056/NEJMra0706596
10. Coffelt SB, Lewis CE, Naldini L, Brown JM, Ferrara N, De Palma M (2010) Elusive identities and overlapping phenotypes of proangiogenic myeloid cells in tumors. Am J Pathol 176(4):1564–1576. doi:10.2353/ajpath.2010.090786
11. Hanahan D, Coussens LM (2012) Accessories to the crime: functions of cells recruited to the tumor microenvironment. Cancer Cell 21(3):309–322. doi:10.1016/j.ccr.2012.02.022
12. Bergers G, Benjamin LE (2003) Tumorigenesis and the angiogenic switch. Nat Rev Cancer 3(6):401–410. doi:10.1038/nrc1093
13. Erdag G, Schaefer JT, Smolkin ME, Deacon DH, Shea SM, Dengel LT, Patterson JW, Slingluff CL Jr (2012) Immunotype and immunohistologic characteristics of tumor-infiltrating immune cells are associated with clinical outcome in metastatic melanoma. Cancer Res 72(5):1070–1080. doi:10.1158/0008-5472.CAN-11-3218
14. Galon J, Costes A, Sanchez-Cabo F, Kirilovsky A, Mlecnik B, Lagorce-Pages C, Tosolini M, Camus M, Berger A, Wind P, Zinzindohoue F, Bruneval P, Cugnenc PH, Trajanoski Z, Fridman WH, Pages F (2006) Type, density, and location of immune cells within human colorectal tumors predict clinical outcome. Science 313(5795):1960–1964. doi:10.1126/science.1129139
15. Zhang L, Conejo-Garcia JR, Katsaros D, Gimotty PA, Massobrio M, Regnani G, Makrigiannakis A, Gray H, Schlienger K, Liebman MN, Rubin SC, Coukos G (2003) Intratumoral T cells, recurrence, and survival in epithelial ovarian cancer. N Engl J Med 348(3):203–213. doi:10.1056/NEJMoa020177
16. Eerola AK, Soini Y, Paakko P (2000) A high number of tumor-infiltrating lymphocytes are associated with a small tumor size, low tumor stage, and a favorable prognosis in operated small cell lung carcinoma. Clin Cancer Res 6(5):1875–1881
17. Robinson BD, Sica GL, Liu YF, Rohan TE, Gertler FB, Condeelis JS, Jones JG (2009) Tumor microenvironment of metastasis in human breast carcinoma: a potential prognostic marker linked to hematogenous dissemination. Clin Cancer Res 15(7):2433–2441. doi:10.1158/1078-0432.CCR-08-2179
18. de Visser KE, Eichten A, Coussens LM (2006) Paradoxical roles of the immune system during cancer development. Nat Rev Cancer 6(1):24–37. doi:10.1038/nrc1782
19. Balkwill F, Charles KA, Mantovani A (2005) Smoldering and polarized inflammation in the initiation and promotion of malignant disease. Cancer Cell 7(3):211–217. doi:10.1016/j.ccr.2005.02.013
20. Hanahan D, Weinberg RA (2011) Hallmarks of cancer: the next generation. Cell 144(5):646–674. doi:10.1016/j.cell.2011.02.013
21. Benelli R, Morini M, Carrozzino F, Ferrari N, Minghelli S, Santi L, Cassatella M, Noonan DM, Albini A (2002) Neutrophils as a key cellular target for angiostatin: implications for regulation of angiogenesis and inflammation. FASEB J 16(2):267–269. doi:10.1096/fj.01-0651fje
22. Nozawa H, Chiu C, Hanahan D (2006) Infiltrating neutrophils mediate the initial angiogenic switch in a mouse model of multistage carcinogenesis. Proc Natl Acad Sci USA 103(33):12493–12498. doi:10.1073/pnas.0601807103
23. Mantovani A, Sica A (2010) Macrophages, innate immunity and cancer: balance, tolerance, and diversity. Curr Opin Immunol 22(2):231–237. doi:10.1016/j.coi.2010.01.009
24. Ribatti D, Vacca A, Nico B, Crivellato E, Roncali L, Dammacco F (2001) The role of mast cells in tumour angiogenesis. Br J Haematol 115(3):514–521
25. De Palma M, Venneri MA, Galli R, Sergi Sergi L, Politi LS, Sampaolesi M, Naldini L (2005) Tie2 identifies a hematopoietic lineage of proangiogenic monocytes required for tumor vessel formation and a mesenchymal population of pericyte progenitors. Cancer Cell 8(3):211–226. doi:10.1016/j.ccr.2005.08.002
26. Lewis CE, De Palma M, Naldini L (2007) Tie2-expressing monocytes and tumor angiogenesis: regulation by hypoxia and angiopoietin-2. Cancer Res 67(18):8429–8432. doi:10.1158/0008-5472.CAN-07-1684
27. Gottfried E, Kreutz M, Haffner S, Holler E, Iacobelli M, Andreesen R, Eissner G (2007) Differentiation of human tumour-associated dendritic cells into endothelial-like cells: an alternative pathway of tumour angiogenesis. Scand J Immunol 65(4):329–335. doi:10.1111/j.1365-3083.2007.01903.x
28. Purhonen S, Palm J, Rossi D, Kaskenpaa N, Rajantie I, Yla-Herttuala S, Alitalo K, Weissman IL, Salven P (2008) Bone marrow-derived circulating endothelial precursors do not contribute to vascular endothelium and are not needed for tumor growth. Proc Natl Acad Sci USA 105(18):6620–6625. doi:10.1073/pnas.0710516105
29. Zumsteg A, Baeriswyl V, Imaizumi N, Schwendener R, Ruegg C, Christofori G (2009) Myeloid cells contribute to tumor lymphangiogenesis. PLoS One 4(9):e7067. doi:10.1371/journal.pone.0007067
30. Ferrara N, Hillan KJ, Gerber HP, Novotny W (2004) Discovery and development of bevacizumab, an anti-VEGF antibody for treating cancer. Nat Rev Drug Discov 3(5):391–400. doi:10.1038/nrd1381
31. Han ES, Burger RA, Darcy KM, Sill MW, Randall LM, Chase D, Parmakhtiar B, Monk BJ, Greer BE, Connelly P, Degeest K, Fruehauf JP (2010) Predictive and prognostic angiogenic markers in a gynecologic oncology group phase II trial of bevacizumab in recurrent and persistent ovarian or peritoneal cancer. Gynecol Oncol 119(3):484–490. doi:10.1016/j.ygyno.2010.08.016
32. Sandler A, Gray R, Perry MC, Brahmer J, Schiller JH, Dowlati A, Lilenbaum R, Johnson DH (2006) Paclitaxel-carboplatin alone or with bevacizumab for non-small-cell lung cancer. N Engl J Med 355(24):2542–2550. doi:10.1056/NEJMoa061884
33. Bergers G, Hanahan D (2008) Modes of resistance to anti-angiogenic therapy. Nat Rev Cancer 8(8):592–603. doi:10.1038/nrc2442
34. Chung AS, Wu X, Zhuang G, Ngu H, Kasman I, Zhang J, Vernes JM, Jiang Z, Meng YG, Peale FV, Ouyang W, Ferrara N (2013) An interleukin-17-mediated paracrine network promotes tumor resistance to anti-angiogenic therapy. Nat Med 19(9):1114–1123. doi:10.1038/nm.3291
35. Vasudev NS, Reynolds AR (2014) Anti-angiogenic therapy for cancer: current progress, unresolved questions and future directions. Angiogenesis 17(3):471–494. doi:10.1007/s10456-014-9420-y

36. Wehland M, Bauer J, Magnusson NE, Infanger M, Grimm D (2013) Biomarkers for anti-angiogenic therapy in cancer. Int J Mol Sci 14(5):9338–9364. doi:10.3390/ijms14059338
37. Asahara T, Murohara T, Sullivan A, Silver M, van der Zee R, Li T, Witzenbichler B, Schatteman G, Isner JM (1997) Isolation of putative progenitor endothelial cells for angiogenesis. Science 275(5302):964–967
38. Blann AD, Woywodt A, Bertolini F, Bull TM, Buyon JP, Clancy RM, Haubitz M, Hebbel RP, Lip GY, Mancuso P, Sampol J, Solovey A, Dignat-George F (2005) Circulating endothelial cells. Biomarker of vascular disease. Thromb Haemost 93(2):228–235. doi:10.1267/THRO05020228
39. Hanahan D (1985) Heritable formation of pancreatic beta-cell tumours in transgenic mice expressing recombinant insulin/simian virus 40 oncogenes. Nature 315(6015):115–122
40. Guy CT, Cardiff RD, Muller WJ (1992) Induction of mammary tumors by expression of polyomavirus middle T oncogene: a transgenic mouse model for metastatic disease. Mol Cell Biol 12(3):954–961
41. Lin EY, Jones JG, Li P, Zhu L, Whitney KD, Muller WJ, Pollard JW (2003) Progression to malignancy in the polyoma middle T oncoprotein mouse breast cancer model provides a reliable model for human diseases. Am J Pathol 163(5):2113–2126. doi:10.1016/S0002-9440(10)63568-7
42. Okabe M, Ikawa M, Kominami K, Nakanishi T, Nishimune Y (1997) 'Green mice' as a source of ubiquitous green cells. FEBS Lett 407(3):313–319
43. Foster BA, Gingrich JR, Kwon ED, Madias C, Greenberg NM (1997) Characterization of prostatic epithelial cell lines derived from transgenic adenocarcinoma of the mouse prostate (TRAMP) model. Cancer Res 57(16):3325–3330
44. Waldmeier L, Meyer-Schaller N, Diepenbruck M, Christofori G (2012) Py2T murine breast cancer cells, a versatile model of TGFbeta-induced EMT in vitro and in vivo. PLoS One 7(11):e48651. doi:10.1371/journal.pone.0048651
45. Aslakson CJ, Miller FR (1992) Selective events in the metastatic process defined by analysis of the sequential dissemination of subpopulations of a mouse mammary tumor. Cancer Res 52(6):1399–1405
46. Lehembre F, Yilmaz M, Wicki A, Schomber T, Strittmatter K, Ziegler D, Kren A, Went P, Derksen PW, Berns A, Jonkers J, Christofori G (2008) NCAM-induced focal adhesion assembly: a functional switch upon loss of E-cadherin. EMBO J 27(19):2603–2615. doi:10.1038/emboj.2008.178
47. Fantozzi A, Gruber DC, Pisarsky L, Heck C, Kunita A, Yilmaz M, Meyer-Schaller N, Cornille K, Hopfer U, Bentires-Alj M, Christofori G (2014) VEGF-mediated angiogenesis links EMT-induced cancer stemness to tumor initiation. Cancer Res 74(5):1566–1575. doi:10.1158/0008-5472.CAN-13-1641
48. Benard A, Ceredig R, Rolink AG (2006) Regulatory T cells control autoimmunity following syngeneic bone marrow transplantation. Eur J Immunol 36(9):2324–2335. doi:10.1002/eji.200636434
49. Wood JM, Bold G, Buchdunger E, Cozens R, Ferrari S, Frei J, Hofmann F, Mestan J, Mett H, O'Reilly T, Persohn E, Rosel J, Schnell C, Stover D, Theuer A, Towbin H, Wenger F, Woods-Cook K, Menrad A, Siemeister G, Schirner M, Thierauch KH, Schneider MR, Drevs J, Martiny-Baron G, Totzke F (2000) PTK787/ZK 222584, a novel and potent inhibitor of vascular endothelial growth factor receptor tyrosine kinases, impairs vascular endothelial growth factor-induced responses and tumor growth after oral administration. Cancer Res 60(8):2178–2189
50. Schomber T, Zumsteg A, Strittmatter K, Crnic I, Antoniadis H, Littlewood-Evans A, Wood J, Christofori G (2009) Differential effects of the vascular endothelial growth factor receptor inhibitor PTK787/ZK222584 on tumor angiogenesis and tumor lymphangiogenesis. Mol Cancer Ther 8(1):55–63. doi:10.1158/1535-7163.MCT-08-0679
51. Hilberg F, Roth GJ, Krssak M, Kautschitsch S, Sommergruber W, Tontsch-Grunt U, Garin-Chesa P, Bader G, Zoephel A, Quant J, Heckel A, Rettig WJ (2008) BIBF 1120: triple angiokinase inhibitor with sustained receptor blockade and good antitumor efficacy. Cancer Res 68(12):4774–4782. doi:10.1158/0008-5472.CAN-07-6307
52. Casanovas O, Hicklin DJ, Bergers G, Hanahan D (2005) Drug resistance by evasion of antiangiogenic targeting of VEGF signaling in late-stage pancreatic islet tumors. Cancer Cell 8(4):299–309. doi:10.1016/j.ccr.2005.09.005
53. Paez-Ribes M, Allen E, Hudock J, Takeda T, Okuyama H, Vinals F, Inoue M, Bergers G, Hanahan D, Casanovas O (2009) Antiangiogenic therapy elicits malignant progression of tumors to increased local invasion and distant metastasis. Cancer Cell 15(3):220–231. doi:10.1016/j.ccr.2009.01.027
54. Crnic I, Strittmatter K, Cavallaro U, Kopfstein L, Jussila L, Alitalo K, Christofori G (2004) Loss of neural cell adhesion molecule induces tumor metastasis by up-regulating lymphangiogenesis. Cancer Res 64(23):8630–8638. doi:10.1158/0008-5472.CAN-04-2523
55. Compagni A, Wilgenbus P, Impagnatiello MA, Cotten M, Christofori G (2000) Fibroblast growth factors are required for efficient tumor angiogenesis. Cancer Res 60(24):7163–7169
56. Fraley CaR A (2002) Model-based clustering, discriminant analysis and density estimation. J Am Assoc 97:611–631
57. Folkman J, Watson K, Ingber D, Hanahan D (1989) Induction of angiogenesis during the transition from hyperplasia to neoplasia. Nature 339(6219):58–61. doi:10.1038/339058a0
58. De Palma M, Murdoch C, Venneri MA, Naldini L, Lewis CE (2007) Tie2-expressing monocytes: regulation of tumor angiogenesis and therapeutic implications. Trends Immunol 28(12):519–524. doi:10.1016/j.it.2007.09.004
59. Bergers G, Javaherian K, Lo KM, Folkman J, Hanahan D (1999) Effects of angiogenesis inhibitors on multistage carcinogenesis in mice. Science 284(5415):808–812
60. Compagni A, Christofori G (2000) Recent advances in research on multistage tumorigenesis. Br J Cancer 83(1):1–5. doi:10.1054/bjoc.2000.1309
61. Wong SC, Puaux AL, Chittezhath M, Shalova I, Kajiji TS, Wang X, Abastado JP, Lam KP, Biswas SK (2010) Macrophage polarization to a unique phenotype driven by B cells. Eur J Immunol 40(8):2296–2307. doi:10.1002/eji.200940288
62. Hardy RR, Kincade PW, Dorshkind K (2007) The protean nature of cells in the B lymphocyte lineage. Immunity 26(6):703–714. doi:10.1016/j.immuni.2007.05.013
63. LeBien TW, Tedder TF (2008) B lymphocytes: how they develop and function. Blood 112(5):1570–1580. doi:10.1182/blood-2008-02-078071
64. Welner RS, Pelayo R, Kincade PW (2008) Evolving views on the genealogy of B cells. Nat Rev Immunol 8(2):95–106. doi:10.1038/nri2234
65. Allman D, Pillai S (2008) Peripheral B cell subsets. Curr Opin Immunol 20(2):149–157. doi:10.1016/j.coi.2008.03.014
66. Sessa C, Guibal A, Del Conte G, Ruegg C (2008) Biomarkers of angiogenesis for the development of antiangiogenic therapies in oncology: tools or decorations? Nat Clin Pract Oncol 5(7):378–391. doi:10.1038/ncponc1150
67. Mancuso P, Calleri A, Cassi C, Gobbi A, Capillo M, Pruneri G, Martinelli G, Bertolini F (2003) Circulating endothelial cells as a novel marker of angiogenesis. Adv Exp Med Biol 522:83–97
68. Pircher A, Hilbe W, Heidegger I, Drevs J, Tichelli A, Medinger M (2011) Biomarkers in tumor angiogenesis and anti-angiogenic therapy. Int J Mol Sci 12(10):7077–7099. doi:10.3390/ijms12107077

69. DeNardo DG, Barreto JB, Andreu P, Vasquez L, Tawfik D, Kolhatkar N, Coussens LM (2009) CD4(+) T cells regulate pulmonary metastasis of mammary carcinomas by enhancing protumor properties of macrophages. Cancer Cell 16(2):91–102. doi:10.1016/j.ccr.2009.06.018
70. Carsetti R, Rosado MM, Wardmann H (2004) Peripheral development of B cells in mouse and man. Immunol Rev 197:179–191
71. Stockmann C, Schadendorf D, Klose R, Helfrich I (2014) The impact of the immune system on tumor: angiogenesis and vascular remodeling. Front Oncol 4:69. doi:10.3389/fonc.2014.00069
72. Nelson BH (2010) $CD20^{+}$ B cells: the other tumor-infiltrating lymphocytes. J Immunol 185(9):4977–4982. doi:10.4049/jimmunol.1001323
73. Mantovani A (2011) B cells and macrophages in cancer: yin and yang. Nat Med 17(3):285–286. doi:10.1038/nm0311-285
74. de Visser KE, Korets LV, Coussens LM (2005) De novo carcinogenesis promoted by chronic inflammation is B lymphocyte dependent. Cancer Cell 7(5):411–423. doi:10.1016/j.ccr.2005.04.014
75. Schioppa T, Moore R, Thompson RG, Rosser EC, Kulbe H, Nedospasov S, Mauri C, Coussens LM, Balkwill FR (2011) B regulatory cells and the tumor-promoting actions of TNF-alpha during squamous carcinogenesis. Proc Natl Acad Sci USA 108(26):10662–10667. doi:10.1073/pnas.1100994108
76. Yang C, Lee H, Pal S, Jove V, Deng J, Zhang W, Hoon DS, Wakabayashi M, Forman S, Yu H (2013) B cells promote tumor progression via STAT3 regulated-angiogenesis. PLoS One 8(5):e64159. doi:10.1371/journal.pone.0064159
77. Zhang X (2013) Regulatory functions of innate-like B cells. Cell Mol Immunol 10(2):113–121. doi:10.1038/cmi.2012.63
78. Newton DJ, Kennedy G, Chan KK, Lang CC, Belch JJ, Khan F (2012) Large and small artery endothelial dysfunction in chronic fatigue syndrome. Int J Cardiol 154(3):335–336. doi:10.1016/j.ijcard.2011.10.030
79. Hamm A, Veschini L, Takeda Y, Costa S, Delamarre E, Squadrito ML, Henze AT, Wenes M, Serneels J, Pucci F, Roncal C, Anisimov A, Alitalo K, De Palma M, Mazzone M (2013) PHD2 regulates arteriogenic macrophages through TIE2 signalling. EMBO Mol Med 5(6):843–857. doi:10.1002/emmm.201302695
80. Takeda Y, Costa S, Delamarre E, Roncal C, Leite de Oliveira R, Squadrito ML, Finisguerra V, Deschoemaeker S, Bruyere F, Wenes M, Hamm A, Serneels J, Magat J, Bhattacharyya T, Anisimov A, Jordan BF, Alitalo K, Maxwell P, Gallez B, Zhuang ZW, Saito Y, Simons M, De Palma M, Mazzone M (2011) Macrophage skewing by Phd2 haplodeficiency prevents ischaemia by inducing arteriogenesis. Nature 479(7371):122–126. doi:10.1038/nature10507
81. Meyer M, Clauss M, Lepple-Wienhues A, Waltenberger J, Augustin HG, Ziche M, Lanz C, Buttner M, Rziha HJ, Dehio C (1999) A novel vascular endothelial growth factor encoded by Orf virus, VEGF-E, mediates angiogenesis via signalling through VEGFR-2 (KDR) but not VEGFR-1 (Flt-1) receptor tyrosine kinases. EMBO J 18(2):363–374. doi:10.1093/emboj/18.2.363
82. Lyttle DJ, Fraser KM, Fleming SB, Mercer AA, Robinson AJ (1994) Homologs of vascular endothelial growth factor are encoded by the poxvirus orf virus. J Virol 68(1):84–92
83. Mestas J, Hughes CC (2004) Of mice and not men: differences between mouse and human immunology. J Immunol 172(5):2731–2738